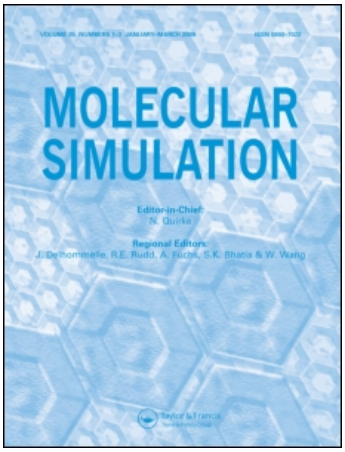

Molecular Simulation
Publication details, including instructions for authors and subscription information:
http://www.informaworld.com/smpp/title~content=t713644482

Thermodynamic and Structural Properties of 1M, 2M and 3M Mixtures of Primitive Model Electrolytes at 25°C with a Common Ion, One counterion of the Same Size, the Other Larger

Torben Smith Sørensen[ab]; Vicente Compañ[c]
[a] Physical Chemistry, Modelling and Thermodynamics, Vanløe, Denmark [b] Universitat Jaume 1, caslón, Spain [c] Departamento de Ciéncias Experimentales, Universitat Jaume 1, caslón, Spain

To cite this Article Sørensen, Torben Smith and Compañ, Vicente(1996) 'Thermodynamic and Structural Properties of 1M, 2M and 3M Mixtures of Primitive Model Electrolytes at 25°C with a Common Ion, One counterion of the Same Size, the Other Larger', Molecular Simulation, 18: 4, 225 — 275
To link to this Article: DOI: 10.1080/08927029608022361
URL: http://dx.doi.org/10.1080/08927029608022361

Molecular Simulation, 1996, Vol. 18, pp. 225–275
Reprints available directly from the publisher
Photocopying permitted by license only

THERMODYNAMIC AND STRUCTURAL PROPERTIES OF 1M, 2M AND 3M MIXTURES OF PRIMITIVE MODEL ELECTROLYTES AT 25°C WITH A COMMON ION, ONE COUNTERION OF THE SAME SIZE, THE OTHER LARGER

TORBEN SMITH SØRENSEN[a] and VICENTE COMPAÑ[b]

[a]Physical Chemistry, Modelling and Thermodynamics, D TH, Nørager Plads 3, DK 2720, Vanløse, Denmark, [b]Departamento de Ciéncias Experimentales, Universitat Jaume 1, E12080 Castellón Spain

(Received June 1996, accepted June 1996)

Using canonical ensemble Monte Carlo simulations in combination with the Widom test particle technique corrected for deviations from electroneutrality we have calculated excess free energies, excess heat capacities at constant volume, single ion activity coefficients, excess osmotic coefficients and radial distribution functions at constant total salt concentration for a mixture of primitive model electrolytes with a common ion. The monovalent, common ion (for brevity called K^+) and the monovalent counterion no. 1 (called Cl^-) have the same diameter, whereas the diameter for the monovalent counterion no. 2 (called F^-) is larger (strongly hydrated ion). The conditions of the simulation correspond to a 3 mol/L total salt concentration in a dielectric continuum as water at 25°C, if the diameters d_{K^+} and d_{Cl^-} are set to 0.29 nm and the diameter d_{F^-} to 0.37 nm. Linear Harned laws of variation with the salt fraction is found for the logarithms of the activity coefficients (ln y) as well as for the other thermodynamic parameters. The variation of ln y_{K^+} with salt fraction is much greater than the variations of ln y_{Cl^-} and ln y_{F^-}. From the radial distribution functions we calculate the potential of mean force between the ions and the mean electric potential around each ion. Near to contact, the Debye-Hückel potential is a fair approximation to the potentials of mean force between all ions, but the electric potentials have to be fitted by Debye-Hückel expressions using individual screening lengths for each ion which are shorter than the Debye length. A comparison is made between the values obtained in the present study and the values obtained in earlier studies at 1 mol/L and 2 mol/L total concentrations and with values obtained by the MSA theory. A general theory for the variation of the Harned coefficients with the total concentration in terms

[a]Guest professor at Universitat Jaume 1, Castellón, Spain, until September 1997.

of the concentration dependence of the activity coefficients of the pure salt solutions is proposed. It is shown that the latter dependence is an Åkerlöf-Thomas relation and that the Harned coefficients are almost independent of the total concentration which implies, that the trace activity coefficient of the two salts are almost identical at the same total concentration.

Keywords: Canonical ensemble Monte Carlo, primitive model KCl-KF mixtures at 1,2 and 3 M, excess energy, heat capacity, single ion activity coefficients, osmotic pressure, Harned rules, potentials of mean forces, electric potentials, MSA theory.

INTRODUCTION

There have only been a few Monte Carlo simulations of ternary ionic solutions in the literature. Based on approximate calculations from experimental electromotive force data [1–3], simulations of 1 M and 2 M primitive model electrolyte mixtures (at the permittivity of water and 25°C) have been reported alone or together with other results [3–8]. In these studies there was one common cation of diameter 0.29 nm, one anion of diameter 0.29 nm and one anion of diameter 0.34 nm or 0.37 nm. For easy reference these systems have been called a "normal" and an "exaggerated" KCl/KF system.

In real aqueous solutions the effective size of the fluoride ion is greater than the sizes of the potassium and the chloride ions, since the small F^- ion is more hydrated (hydrogen bonds) than the K^+ and the Cl^- ions. From emf measurements [1–3] it is quite difficult to observe the difference between the mean activity coefficients of KCl and KF in mixtures at the same ionic strength, and the effective diameter 0.34 nm of the fluoride ion is probably more realistic than the diameter 0.37 nm. In emf studies with concentration cells involving a cellulose acetate membrane, a much better discrimination between F^- and Cl^- is obtained due to diffusion of the hydrated ions in narrow channels [9]. The "exaggerated" KCl/KF system serves the purpose of showing more clearly the effect of size in simulations of a ternary electrolyte system with one common monovalent cation, one monovalent anion with the same size and another monovalent anion, which is larger.

In the present study we concentrate exclusively on the Canonical Ensemble Monte Carlo simulation of a 3 M "exaggerated" KCl/KF solution. The purpose is to investigate the linear Harned rules for the thermodynamic parameters by comparison with the studies of the same system at 1 M and 2 M. Furthermore, an object is to investigate the radial distribution functions, the "potentials of mean forces" between the

ions and the mean electric potentials around each type of ion in the mixture.

METHODOLOGY

The Canonical Ensemble Monte Carlo simulations were basically performed using the method of Metropolis *et al.* [10] using periodic boundary conditions and "minimum image" energy cut-off as in the original work of Card and Valleau [11]. Sampling the configurational energies in the stochastic Markov process established by the Metropolis rules, an estimate of the excess internal energy (E_{ex}) is calculated. From the variance of the fluctuations in the configurational energy the excess heat capacity at constant volume ($C_{V,ex}$) is calculated.

The numbers of the two kind of anions in the basic simulation cell are selected, and from the principle of electroneutrality follows the number of cations and the total number of ions (N). These ions were placed randomly and/or in a lattice in a non-overlapping configuration in the basic cell and the simulation process was started. The first 30,000 configurations were always omitted in order to "equilibrate" the Markov process. The random number generator is used for other purposes than for the central Metropolis selection of rejection or no rejection of the preceding "move of game". It is used for specifying which one of the ions should be moved next, and how long it should move in the three directions. This is done by randomly selecting the fraction of the maximum distance an ion should be moved in each direction. This maximum distance is specified by the dimensionless parameter d given by:

$$d = \text{maximum coordinate change for a ion}/L \tag{1}$$

where L is the dimensionless length of the basic (cubic) simulation cell (measured in terms of the mean diameter of the ions a). In all the simulations reported previously we have used $d = 0.5$, since if an ion is moved more than one half cell length in one direction, the same situation is generated as with a shorter displacement due to the periodic boundary conditions. However, in order to create even more variation in the simulations, we have in the present study chosen different values of $d \leqslant 0.5$.

The strength of the electrostatic interaction compared to the kinetic energy of the particles is for the primitive electrolyte model given by the

dimensionless Bjerrum parameter

$$B \equiv e_0^2/(4\pi\varepsilon\, kTa) \equiv \lambda_B/a \tag{2}$$

where e_0 is the unit charge, ε the dielectric permittivity of the solvent treated as a continuum, k is the Boltzmann constant, T the absolute temperature, a the mean diameter of the three ions (or of the two ions in the two ion systems) and λ_B the Bjerrum length. All distances are measured relative to the mean diamter a, for example the separation between ion i and ion j:

$$t_{ij} = r_{ij}/a \tag{3}$$

For hard, charged spheres in a dielectric continuum the dimensionless Hamiltonion pair potential between ion i and ion j is then given by

$$U_{ij}/kT = z_i z_j B/t_{ij}\,(t_{ij} \geqslant a_{ij}/a); \quad U_{ij}/kT = \infty\ (t_{ij} < a_{ij}/a) \tag{4}$$

where z_i and z_j are the valencies (with sign) of the two ions and a_{ij} the contact distance between the two ions (mean diameter of this pair of ions). The total salt concentration (ρ) may be expressed as a dimensionless quantitiy multiplying the total particle density by a^3:

$$\rho^* \equiv \rho a^3 \tag{5}$$

In water at 25 °C the Bjerrum length is ca. 0.71 nm. In this study it was set to $\lambda_B = 0.71554$ nm. The ionic diameters were 0.29 nm for K^+ and Cl^- and 0.37 for (exaggerated) F^-. For solutions of 3 M total salt concentration at 25 °C we then have:

$$\text{Pure KCl:} \quad a = 0.29\ \text{nm}, \quad B = 2.4605, \quad \rho^* = 0.08814 \tag{6a}$$

$$\text{Pure KF:} \quad a = 0.33\ \text{nm}, \quad B = 2.16225, \quad \rho^* = 0.12987 \tag{6b}$$

$$\text{Mixed KCl/KF:} \quad a = 0.31666\ldots\text{nm}, \quad B = 2.2533, \quad \rho^* = 0.11475 \tag{6c}$$

Apart from the much longer simulation runs and the application of higher numbers of ions, the main difference between the methods of this and the previous papers and the methods of the classical work of Card and Valleau [11] lies in the extrapolation to the thermodynamic limit ("infinite" thermodynamic system) of the thermodynamic quantities. It was shown many times that the $1/N$ extrapolation to $1/N = 0$ used by these and later authors

was not correct. In fact, the first term is not to the order $1/N$ but to the order $(1/N)^{2/3}$. Therefore, extrapolating with the first term as $1/N$ makes the extrapolation singular in $(1/N)=0$.

In dilute systems of two ions with equal diameter at moderate Bjerrum parameters, a "universal" scaling was found (independent of B and ρ^*, see references [12–13]) in terms of the parameter.

$$x \equiv 2/(L\kappa a) \tag{7}$$

which may be thought of as the Debye length (κ^{-1}) divided by half the edge length of the simulation cell ($La/2$). This is a measure of the deviation from the "thermodynamic limit". For example, E_{ex}/NkT divided by the same quantity in the thermodynamic limit could be expressed as a "universal" polynomial in x starting with x^2:

$$\begin{aligned}(E_{ex}/NkT)/\lim_{N\to\infty}(E_{ex}/NkT) = 1 + 0.152526x^2 \\ + 0.783555x^3 - 0.45261x^4\end{aligned} \tag{8}$$

Since we have

$$\kappa a = (4\pi B\rho^*)^{1/2} \tag{9}$$

and since B and ρ^* are constant in a series with varying N, κa is constant. Furthermore, $L=(N/\rho^*)^{1/3}$ and x^2 is proportional to $(1/N)^{2/3}$. In non-dilute systems, there is no "universal" scaling, but instead quite perfect linear extrapolations in x^2 are often seen, so that for example E_{ex}/NkT plotted *vs.* $(1/N)^{2/3}$ made a perfect straight line for values of N varying from 16 to 1000 or more. As an example, see ref. [8], Figure 1.

Another difference with the work of previous authors is that estimates for the single ion excess chemical potentials divided by kT (the logarithm of the single ion activity) are found directly during the simulation runs. The method used is the "test particle" method invented by Widom [14–15]. This method is based on the relation between the excess Helmholtz free energy F_{ex} and the configuration integral Z. One has the following approximation

$$\mu_i/kT - \mu_{o,i}/kT \approx -\ln(Z_{N+1}/Z_N) \tag{10}$$

where the additional ion in the numerator on the right hand side is of type i and $\mu_{0,i}/kT$ is the standard chemical potential of the ion. The approximation in Eq. (10) is good for large values on N. It is easy to demonstrate

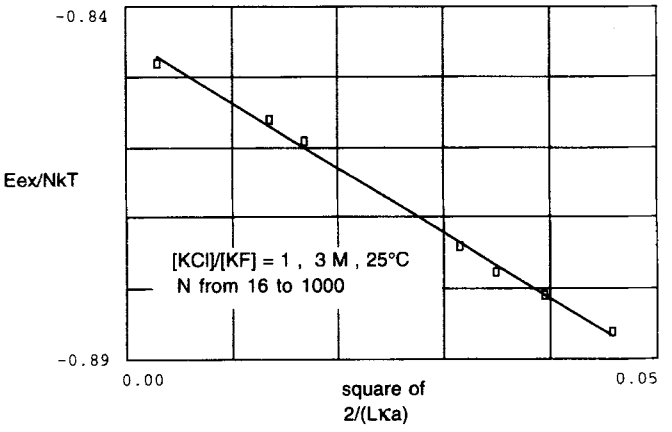

FIGURE 1 The dimensionless excess energy per ion as a function of $[2/(L\kappa a)]^2$ for an equimolar mixture of KCl and KF at 3 mol/L total concentration (25°C).

that we can rewrite Eq. (10) as:

$$\mu_i/kT - \mu_{0,i}/kT \approx -\ln(V/N_i + 1) - \ln\langle \exp(-U_{\text{test},i}/kT)\rangle \qquad (11)$$

where $\langle\cdots\rangle$ signifies averaging over the canonical ensemble (the Markov process), V is the volume of the system and $U_{\text{test},i}$ is the energy of a fixed "test ion" of type i relative to all the other "real ions" in the simulation cell. For large values of N_i we have

$$\ln(V/N_i + 1) \approx \ln(V/N_i) = -\mu_{\text{ideal},i}/kT$$

where $\mu_{\text{ideal},i}$ is the ideal, concentration dependent part of the chemical potential for ion i(no interaction). Thus, we can write for the "excess chemical potentials" (the logarithm of the single ion activity coefficient):

$$\ln y_i \equiv \mu_{\text{ex},i}/kT \equiv \mu_i/kT - \mu_{0,i}/kT - \mu_{\text{ideal},i}/kT \approx -\ln\langle \exp(-U_{\text{test},i}/kT)\rangle \quad (12)$$

Introduction of test particles does not in any way perturb the normal Metropolis process. The "real particles" freely passes through the hard sphere test particles. In passing the "test energy" is infinite, but since the values of $\exp(-U_{\text{test},i}/kT)$ are sampled, we just have to count one zero whenever overlap occurs. Thus, the test particle method may also be used to calculate the activity coefficients in mixtures of hard sphere particles. Indeed, in ref. [8] the activity coefficients in "exaggerated" 2 M KCl/KF

mixtures were calculated for charged as well as for uncharged particles. The hard sphere results coincided with the values calculated from Carnahan-Starling expressions.

In the simulations 64 test cations and 64 test anions of the two types have been used, distributed in a lattice in the basic simulation cell. Each test ion counts the interactions between itself and the "real ions" (or their images) in a cubic L-box around the test ion. Averaging over 64 test ions at different positions speeds up convergence of the results. The calculation time compared to simulation without test particles is increased by some 50%.

The results obtained in the above way are the "plain Widom" values. However, the formula (12) is only exact in the limit $N \to \infty$, and therefore extrapolation has to be carried out. It was shown in refs. [16–17] that the N-dependence of the plain Widom values is very strong. The first term is of order $(1/N)^{1/3}$ rather than of order $(1/N)^{2/3}$. If $\ln y_i$ is plotted *vs.* $(1/N)^{1/3}$ in non-dilute systems of 1:1 electrolytes with N even and odd, respectively, one obtains approximately two different straight lines extrapolating, however, to practically the same value, when $N \to \infty$, see ref. [17] Figure 1. Thus, deviation from electroneutrality seems to have a lot to do with the slope of the extrapolation plots. It has shown expedient to introduce a continuous background charge in the simulation cell compensating for the charge of the test particle. The correction of the plain Widom values can be calculated analytically, see refs. [13] and [18] for general formulae adding a test particle of any valency to electroneutral as well as nonelectroneutral basic simulation

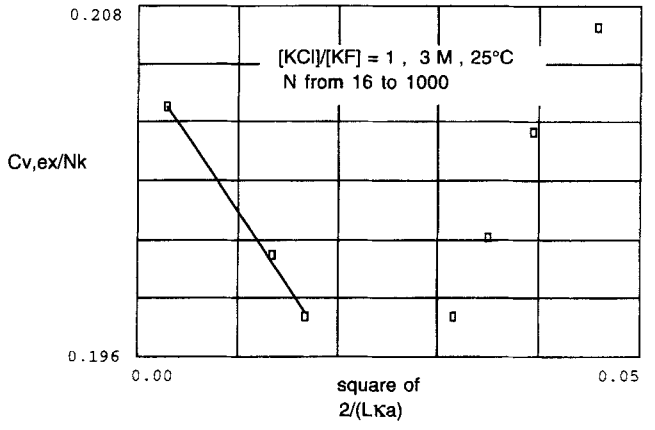

FIGURE 2 The dimensionless excess heat capacity at constant volume per ion as a function of $[2/(L\kappa a)]^2$ for an equimolar mixture of KCl and KF at 3 mol/L total concentration (25°C). The values for the four smallest numbers of ions (N) are nothing worth for the extrapolation.

cells. Here we only state the formula for electroneutral cells and univalent electrolytes:

$$\ln y_i(\text{corr}) = \ln y_i(\text{plain Widom}) - \mathrm{B}\cdot\mathrm{K}/(8\mathrm{L}) \;;\; K \equiv 12\ln(2+\sqrt{3}) - 2\pi \quad (13)$$

The corrected values $\ln y_i$(corr) extrapolate with $(1/N)^{2/3}$ (*i.e.* x^2) as the leading term. The slope is small and the extrapolation distance is short compared to the uncorrected case. In nondilute systems a straight line is often observed, see for example ref. [8] Figure 3 with N from 16 to 1728.

The radial distribution functions [RDF's, $g_{ij}(t)$] were sampled around each ion in the simulation cell and an average was made for each type of ion. The ions of the type in question (of type j) were counted in 60 equidistant spherical shells ($\Delta t = 0.05$) from the minimum contact distance t_{ij}(min) to t_{ij}(max) = 3.00 + t_{ij}(min). The counts were then divided by the bulk concentration of the ion counted. The radial distribution functions thus calculated are systematically too low for N finite in the case of RDF's between identical ions $g_{ii}(t)$, since the central ion is excepted from the counts. The central ion of type i therefore "sees" a dimensionless bulk concentration of i-ions of only $(N_i - 1)/L^3$ instead of N_i/L^3. Since division with the latter is made in the programme, the preliminary output for $g_{ij}(t)$ have to be multiplied by $N_i/(N_i - 1)$. There is no correction for $g_{ij}(t)$ when $j \neq i$. The necessity of this correction was seen very clearly when the RDF's of chargeless "ions" were studied using the same programme, ref. [8], Figures 35–36. In

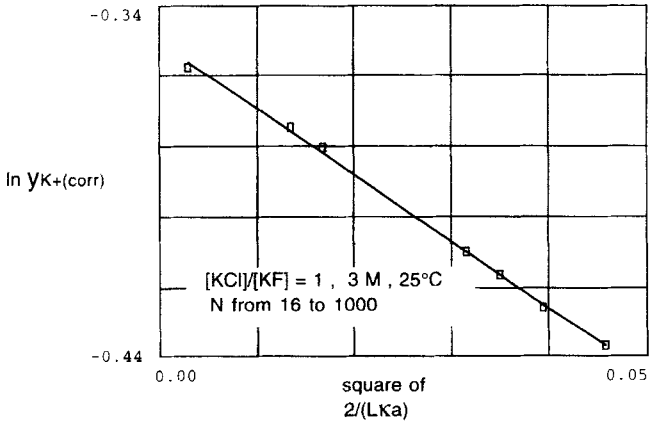

FIGURE 3 The logarithm of the single ion Widom activity coefficients of K^+ corrected to electroneutrality using a continuous background charge as a function of $[2/(L\kappa a)]^2$ for an equimolar mixture of KCl and KF at 3 mol/L total concentration (25 C).

the following we always mean "corrected" $g_{ii}(t)$ when we just write (or plot) $g_{ii}(t)$. The correction is most significant for small systems but does not of course correct for the influence of the periodic boundary conditions and the minimum image energy cut-off in the tail of the RDF's. The RDF's are completely invalid when $t_{ij}(\max) > L/2$.

The "potential of mean force" $W_{ij}(t)$ between two ions is the energy of interaction relative to an infinite separation averaged over all possible positions of the other ions. It is easily shown [19] that the potentials of mean forces can be found directly from the RDF's:

$$\frac{W_{ij}(t)}{kT} = -\ln g_{ij}(t) \tag{14}$$

Thus, when the RDF is greater than unity, the potential is attractive. When it is less than unity it is repulsive.

The mean electric potential $\Psi_k(t)$ around an ion of type k can be obtained from the mean charge density profile around the ion (calculated from the RDF's) integrating numerically the law of Poisson as explained in ref. [6]. One can only find the potential difference $[\Delta\Psi_k(t)]$ relative to a fixed distance from the central ion $t_{\max}$. This distance should be taken to be as large as possible, but should not be in a point of the RDF tail which is affected by the periodic boundary conditions and the energy cut-off. For a mixture of KCl and KF with salt fraction X_{KCl} of KCl in the mixture we use Eqs. (14–19) in ref. [6], where care has been taken to account for the discontinuities in the space charge densities. For example, around a K^+ ion there will be an inner zone where there can only be K^+ ions and Cl^- ions followed by an outer zone where there are all three types of ions. At the boundary between the inner and the outer zone appears a space charge discontinuity.

SIMULATED VALUES OF THE THERMODYNAMIC QUANTITIES

In Tables I–VII a survey of the raw data of the simulations are given. Simulations have been performed at 3 M total concentration and the seven salt ratios $[KCl]/[KF] = \infty$, 4, 3, 1, 1/3, 1/4, 0. Each table states the basic input and output (except RDF's) for a fixed salt ratio and varying values for the total number of ions. The uncertainty of a single simulation can be judged from repeated simulations such as $N = 100$ (a and b) and $N = 216$

TABLE I Simulated thermodynamic quantities for pure 3 M KCl at 25°C ($B = 2.4605$, $\rho^* = 0.08814$)

N	E_{ex}/NkT	$C_{V,ex}/Nk$	$\ln\gamma_{K^+}$ (test)	$\ln\gamma_{Cl^-}$ (test)	d	Millions configs.
16	−0.9100	0.2168	−0.02652	−0.02684	0.488	30.0
24	−0.9021	0.2109	−0.07280	−0.07274	0.479	30.0
32	−0.8968	0.2085	−0.1022	−0.1025	0.399	30.0
44	−0.8914	0.2086	−0.1334	−0.1334	0.444	30.0
64	−0.8867	0.2094	−0.1684	−0.1681	0.497	30.0

The ionic diameter are both 0.29 nm ($= a$).

TABLE II Simulated thermodynamic quantities for pure 3 M KF at 25°C ($B = 2.16225$, $\rho^* = 0.12987$)

N	E_{ex}/NkT	$C_{V,ex}/Nk$	$\ln\gamma_{K^+}$ (test)	$\ln\gamma_{F^-}$ (test)	d	Millions configs.
16	−0.8607	0.1982	0.18867	0.30924	0.299	30.0
24	−0.8527	0.1877	0.14421	0.26513	0.3812	30.0
32	−0.8460	0.1829	0.11640	0.23539	0.412	30.0
44	−0.8393	0.1803	0.087466	0.20582	0.368	30.0
64	−0.8337	0.1810	0.054323	0.17199	0.368	30.0
100a	−0.8293	0.1848	0.017882	0.13270	0.485	30.0
100b	−0.8293	0.1857	0.018729	0.13216	0.383	30.0
216a	−0.8245	0.1869	−0.03983	0.074317	0.474	30.0
216b	−0.8246	0.1882	−0.04122	0.074898	0.455	30.0
216c	−0.8249	0.1869	−0.03864	0.075784	0.481	30.0

The ionic diameters are 0.29 nm for K^+ and 0.37 nm for F^-. Mean diameter $a = 0.33$ nm.

TABLE III Simulated thermodynamic quantities for a 3 M 4:1 mixture of KCl and KF at 25°C ($B = 2.253$, $\rho^* = 0.11475$)

N	E_{ex}/NkT	$C_{V,ex}/Nk$	$\ln\gamma_{K^+}$ (test)	$\ln\gamma_{Cl^-}$ (test)	$\ln\gamma_{F^-}$ (test)	d	Millions configs.
20	−0.89625	0.20830	−0.0100520	−0.0462476	0.2226413	0.447	9.00
30	−0.88770	0.20390	−0.0526632	−0.0890612	0.1803963	0.488	12.00
60	−0.87686	0.20533	−0.118683	−0.156728	0.1148323	0.312	30.0
90	−0.87269	0.20587	−0.154610	−0.190530	0.08286440	0.493	15.00
1000	−0.86459	0.20747	−0.299558	−0.340755	−0.0643494	0.472	18.66

The ionic diameters are 0.29 nm for K^+ and Cl^- and 0.37 nm for F^-. Mean diameter $a = 0.31666..$ nm. N is the total number of ions, *e.g.* $N = 1000$ corresponds to 500 K^+, 400 Cl^- and 100 F^-.

TABLE IV Simulated thermodynamic quantities for a 3 M 3:1 mixture of KCl and KF at 25°C ($B = 2.253$, $\rho^* = 0.11475$)

N	E_{ex}/NkT	$C_{V,ex}/Nk$	lny_{K^+} (test)	lny_{Cl^-} (test)	lny_{F^-} (test)	d	Millions Configs.
800	−0.86203	0.21103	−0.281442	−0.329562	−0.0500527	0.455	15.42
880	−0.86168	0.21258	−0.282972	−0.334637	−0.0568243	0.269	30.00
1000	−0.86182	0.21265	−0.289231	−0.335594	−0.0589219	0.500	30.00

The ionic diameters are 0.29 nm for K^+ and Cl^- and 0.37 nm for F^-. Mean diameter $a = 0.31666..$ nm. N is the total number of ions, *e.g.* $N = 1000$ corresponds to 500 K^+, 375 Cl^- and 125 F^-.

TABLE V Simulated thermodynamic quantities for a 3 M 1:1 mixture of KCl and KF at 25°C ($B = 2.253$, $\rho^* = 0.11475$)

N	E_{ex}/NkT	$C_{V,ex}/Nk$	lny_{K^+} (test)	lny_{Cl^-} (test)	lny_{F^-} (test)	d	Millions Configs.
16	−0.88612	0.20729	0.0800637	−0.0099500	0.2694883	0.500	9.00
20	−0.88103	0.20363	0.0540900	−0.0369185	0.2430939	0.339	9.00
24	−0.87783	0.20009	0.0354550	−0.0556036	0.2260698	0.499	12.00
28	−0.87413	0.19739	0.0191209	−0.0719366	0.2895437	0.411	24.06
72	−0.85900	0.19738	−0.0674288	−0.162480	0.1221988	0.399	30.00
100	−0.85599	0.19947	−0.0939389	−0.189485	0.09362311	0.483	9.60
1000	−0.84807	0.20452	−0.227418	−0.332990	−0.0482146	0.470	30.00

The ionic diameters are 0.29 nm for K^+ and Cl^- and 0.37 nm for F^-. Mean diameter $a = 0.31666..$ nm. N is the total number of ions, *e.g.* $N = 1000$ corresponds to 500 K^+, 250 Cl^- and 250 F^-

TABLE VI Simulated thermodynamic quantities for a 3 M 1:3 mixture of KCl and KF at 25°C ($B = 2.253$, $\rho^* = 0.11475$)

N	E_{ex}/NkT	$C_{V,ex}/Nk$	lny_{K^+} (test)	lny_{Cl^-} (test)	lny_{F^-} (test)	d	Millions Configs.
400	−0.83634	0.19610	−0.130595	−0.274772	0.02086541	0.388	15.00
600	−0.83561	0.19477	−0.149625	−0.299586	$-8.392 \cdot 10^{-5}$	0.499	18.00
800	−0.83465	0.19544	−0.168756	−0.308813	−0.0128343	0.411	30.00
1000	−0.83441	0.19776	−0.174210	−0.319800	−0.0222901	0.437	30.00

The ionic diameters are 0.29 nm for K^+ and Cl^- and 0.37 nm for F^-. Mean diameter $a = 0.31666..$ nm. N is the total number of ions, *e.g.* $N = 1000$ corresponds to 500 K^+, 125 Cl^- and 375 F^-.

(a,b and c) in Table II. It can also be judged from the deviations of the single points from the linear extrapolation plots.

Table VIII summarizes the results of the linear regressions for the extrapolation plots. The plots have the general form

$$X = X(N = \infty) + \alpha(2/L\kappa a)^2 \tag{15}$$

where $X = E_{ex}/NkT$, $C_{V,ex}/NK$, ln y_i(corr) or ln $y_\pm$(corr), where y_i(corr) is a single ion activity coefficient (with a neutralising background) and $y_\pm$(corr)

TABLE VII Simulated thermodynamic quantities for a 3 M 1:4 mixture of KCl and KF at 25 °C ($B = 2.253$, $\rho^* = 0.11475$)

N	E_{ex}/NkT	$C_{V,ex}/Nk$	$\ln y_{K^+}$ (test)	$\ln y_{Cl^-}$ (test)	$\ln y_{F^-}$ (test)	d	Millions Configs.
20	−0.86654	0.19720	0.1192295	−0.0248828	0.2677018	0.437	9.00
30	−0.85750	0.18899	0.0785815	−0.0683484	0.2256914	0.294	9.00
40	−0.85195	0.18573	0.0517937	−0.0955194	0.1986805	0.378	12.00
50	−0.84755	0.18586	0.0311790	−0.0118491	0.1765359	0.444	15.00
60	−0.84493	0.18782	0.0148986	−0.136093	0.1607437	0.377	18.00
100	−0.83968	0.19108	−0.0284736	−0.180966	0.1160405	0.487	30.00
1000	−0.83187	0.19541	−0.164819	−0.314924	−0.0158585	0.365	30.00

The ionic diameters are 0.29 nm for K^+ and Cl^- and 0.37 nm for F^-. Mean diameter $a = 0.31666..$ nm. N is the total number of ions, *e.g.* $N = 1000$ corresponds to 500 K^+, 100 Cl^- and 400 F^-.

a corrected mean ionic activity coefficient of a pure salt or of a salt in the mixture. In Table VIII, the slopes α and the Pearson's r coefficients of the regressions are listed. For E_{ex}/NkT, $\ln y_i$(corr) and $\ln y_{\pm}$(corr) all simulated values of N are included in the regressions, but for $C_{V,ex}/Nk$ the smaller values of N have to be omitted, since the fluctuations of the energy in such small systems are relatively larger than the fluctuations in large systems.

We only show the regression plots of the salt ratio [KCl]/[KF] = 1, Figures 1–5. The regressions for E_{ex}/NkT, $\ln y_{K^+}$(corr), $\ln y_{Cl^-}$(corr) and $\ln y_{F^-}$(corr) *vs.* $(2/L\kappa a)^2$ are quite perfect straight lines for values of N from 16 to 1000. For $C_{V,ex}/Nk$ (Fig. 2) it is different, however. The regression line shown is only involving the three highest values $N = 72$, 100 and 1000. For lower N-values the slope is opposite, *i.e.* the heat capacities increase with decreasing size of the system. These data is of no value for the extrapolation. A similar tendency is clearly seen for the $C_{V,ex}/Nk$ data in Tables II and VII, and perhaps in Tables I, III and VI. The same kind of sharp break in the $C_{V,ex}/Nk$ data as seen in Figure 2 was found earlier in connection with the "universal" plot of $[C_{V,ex}/Nk]/[\lim_{N\to\infty}(C_{V,ex}/Nk)]$ *vs.* $x = (2/L\kappa a)$ found for dilute binary electrolytes, see ref. [12], Figure 16, and ref. [13], Figure 2. In that case the "universal" curve had a leading term of order x^2 followed by a term in x^5 producing a sharp break. However, the change of slope was not sufficient to cause the values of $C_{V,ex}/Nk$ to rise again for higher values of x, such as they do in Figure 2 in this paper.

EXTENDED HARNED'S RULES

Figures 6–12 shows linear "Harned plots" for E_{ex}/NkT, $C_{V,ex}/Nk$, $\ln y_{K^+}$(corr), $\ln y_{Cl^-}$(corr), $\ln y_{\pm}(KCl, corr) \equiv [\ln y_{K^+}(corr) + \ln y_{Cl^-}(corr)]/2$,

TABLE VIII Summary of regressions for the thermodynamic quantities

KCl/KF	*Quantities for* $N = \infty$	α	*Pearson's r*	*N values included*
∞	$E_{ex}/NkT = -0.8718 \pm 0.0005$	−0.8482	−0.99785	16,24,32,44,64
∞	$C_{V,ex}/Nk = 0.211 \pm 0.002$	−0.08356	−0.9041	32,44,64
∞	$\ln y_{\pm}(\text{corr}) = -0.4606 \pm 0.0023$	−1.8194	−0.99980	16,24,32,44,64
4	$E_{ex}/NkT = -0.8609 \pm 0.0020$	−0.8818	−0.99745	20,30,60,90,1000
4	$C_{V,ex}/Nk = 0.208 \pm 0.002$	−0.1310	−0.99966	30,60,90,1000
4	$\ln y_{K^+}(\text{corr}) = -0.4226 \pm 0.0020$	−1.6601	−0.99584	20,30,60,90,1000
4	$\ln y_{Cl^-}(\text{corr}) = -0.4625 \pm 0.0040$	−1.5449	−0.98898	20,30,60,90,1000
4	$\ln y_{F^-}(\text{corr}) = -0.1861 \pm 0.0030$	−1.7561	−0.99375	20,30,60,90,1000
4	$\ln y_{\pm}(\text{KCl,corr}) = -0.4426 \pm 0.0030$	−1.6025	−0.99315	20,30,60,90,1000
4	$\ln y_{\pm}(\text{KF,corr}) = -0.3044 \pm 0.0020$	−1.7081	−0.99517	20,30,60,90,1000
3	$E_{ex}/NkT = -0.8605 \pm 0.0015$	−0.4104	−0.5443	800,880,1000
3	$C_{V,ex}/Nk = 0.223 \pm 0.010$	−3.345	−0.8534	800,880,1000
3	$\ln y_{K^+}(\text{corr}) = -0.406 \pm 0.010$	−4.584	−0.7093	800,880,1000
3	$\ln y_{Cl^-}(\text{corr}) = -0.440 \pm 0.010$	−9.025	−0.8277	800,880,1000
3	$\ln y_{F^-}(\text{corr}) = -0.181 \pm 0.010$	−3.008	−0.3861	800,880,1000
3	$\ln y_{\pm}(\text{KCl,corr}) = -0.4230 \pm 0.0010$	−6.804	−0.99348	800,880,1000
3	$\ln y_{\pm}(\text{KF,corr}) = -0.2935 \pm 0.0010$	−3.796	−0.94491	800,880,1000
1	$E_{ex}/NkT = -0.8445 \pm 0.0020$	−0.9245	−0.99816	16,20,24,28,72,100,1000
1	$C_{V,ex}/Nk = 0.206 \pm 0.005$	−0.5049	−0.99826	72,100,1000
1	$\ln y_{K^+}(\text{corr}) = -0.3504 \pm 0.0020$	−1.8896	−0.99922	16,20,24,28,72,100,1000
1	$\ln y_{Cl^-}(\text{corr}) = -0.4529 \pm 0.0050$	−1.5748	−0.99000	16,20,24,28,72,100,1000
1	$\ln y_{F^-}(\text{corr}) = -0.1673 \pm 0.0050$	−1.7027	−0.98972	16,20,24,28,72,100,1000
1	$\ln y_{\pm}(\text{KCl,corr}) = -0.4016 \pm 0.0030$	−1.7322	−0.99636	16,20,24,28,72,100,1000
1	$\ln y_{\pm}(\text{KF,corr}) = -0.2588 \pm 0.0050$	−1.7962	−0.99607	16,20,24,28,72,100,1000
1/3	$E_{ex}/NkT = -0.8320 \pm 0.0030$	−0.8216	−0.98299	400,600,800,1000
1/3	$C_{V,ex}/Nk = 0.198 \pm 0.002$	−0.4511	−0.3751	400,600,800,1000
1/3	$\ln y_{K^+}(\text{corr}) = -0.3045 \pm 0.0030$	−0.4509	−0.2007	400,600,800,1000
1/3	$\ln y_{Cl^-}(\text{corr}) = -0.4474 \pm 0.0030$	−0.9644	−0.4808	400,600,800,1000
1/3	$\ln y_{F^-}(\text{corr}) = -0.1485 \pm 0.0003$	−1.4051	−0.99284	400,600,800,1000
1/3	$\ln y_{\pm}(\text{KCl,corr}) = -0.3760 \pm 0.0010$	−0.7077	−0.7600	400,600,800,1000
1/3	$\ln y_{\pm}(\text{KF,corr}) = -0.2265 \pm 0.0010$	−0.9280	−0.6652	400,600,800,1000
1/4	$E_{ex}/NkT = -0.8252 \pm 0.0050$	−1.0035	−0.94311	20,30,40,50,60,100,1000
1/4	$C_{V,ex}/Nk = 0.197 \pm 0.005$	−0.4728	−0.98870	40,50,60,100,1000
1/4	$\ln y_{K^+}(\text{corr}) = -0.2859 \pm 0.0030$	−1.8107	−0.99232	20,30,40,50,60,100,1000
1/4	$\ln y_{Cl^-}(\text{corr}) = -0.4390 \pm 0.0030$	−1.6109	−0.99597	20,30,40,50,60,100,1000
1/4	$\ln y_{F^-}(\text{corr}) = -0.1395 \pm 0.0020$	−1.7941	−0.99756	20,30,40,50,60,100,1000
1/4	$\ln y_{\pm}(\text{KCl,corr}) = -0.3625 \pm 0.0020$	−1.7108	−0.99470	20,30,40,50,60,100,1000
1/4	$\ln y_{\pm}(\text{KF,corr}) = -0.2127 \pm 0.0020$	−1.8024	−0.99562	20,30,40,50,60,100,1000
0	$E_{ex}/NkT = -0.8164 \pm 0.0010$	−0.9934	−0.99789	16,24,32,44,64,100a-b,216a-c
0	$C_{V,ex}/Nk = 0.1915 \pm 0.0050$	−0.5003	−0.9610	44,64,100a-b,216a-c
0	$\ln y_{K^+}(\text{corr}) = -0.2391 \pm 0.0030$	−1.9175	−0.9954	16,24,32,44,64,100a-b,216a-c
0	$\ln y_{F^-}(\text{corr}) = -0.1261 \pm 0.0030$	−1.7269	−0.9946	16,24,32,44,64,100a-b,216a-c
0	$\ln y_{\pm}(\text{KF,corr}) = -0.1826 \pm 0.0030$	−1.8222	−0.9953	16,24,32,44,64,100a-b,216a-c

$\ln y_{F^-}(\text{corr})$ and $\ln y_{\pm}(\text{KF, corr})$ *vs.* the salt fraction $X_{KF} \equiv [KF]/\{[KF] + [KCl]\}$. The rectangles are the extrapolated values of the thermodynamic parameters and the lines are the following linear regressions

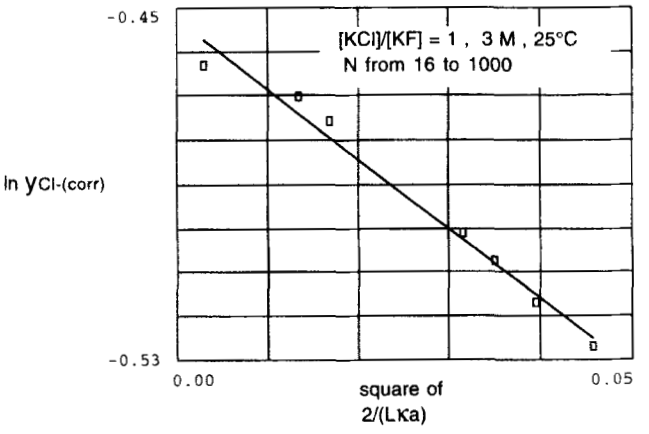

FIGURE 4 The logarithm of the single ion Widom activity coefficients of Cl^- corrected to electroneutrality as a function of $[2/(L\kappa a)]^2$ for an equimolar mixture of KCl and KF at 3 mol/L total concentration (25°C).

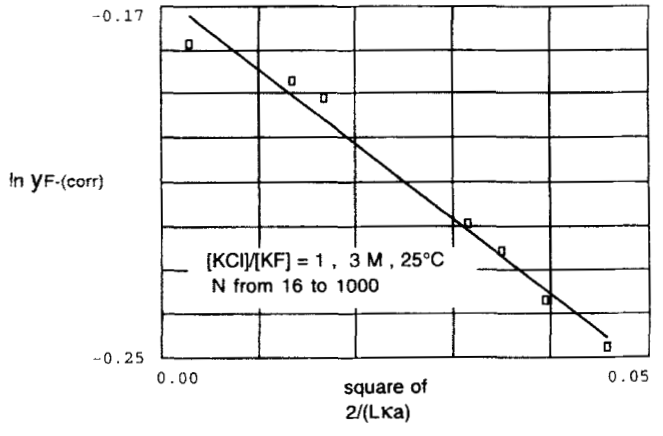

FIGURE 5 The logarithm of the single ion Widom activity coefficients of F^- corrected to electroneutrality as a function of $[2/(L\kappa a)]^2$ for an equimolar mixture of KCl and KF at 3 mol/L total concentration (25°C).

(with estimated uncertainties):

$$E_{ex}/NkT = -0.8728 + 0.05656\, X_{KF} \pm 0.0010\, (r = +0.9975) \qquad (16)$$

$$C_{V,ex}/Nk = -0.217 - 0.0240\, X_{KF} \pm 0.005\, (r = -0.8340) \qquad (17)$$

$$\ln y_{K^+}(\text{corr}) = -0.4628 + 0.2200\, X_{KF} \pm 0.0050\, (r = +0.9989) \qquad (18)$$

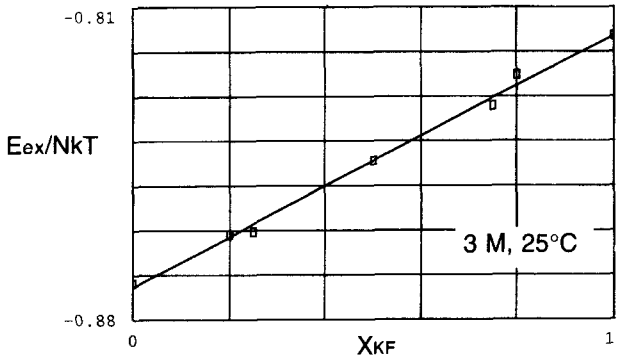

FIGURE 6 Harned plot of the dimensionless excess energy per ion as a function of the fraction of KF at 3 mol/L total concentration (25°C).

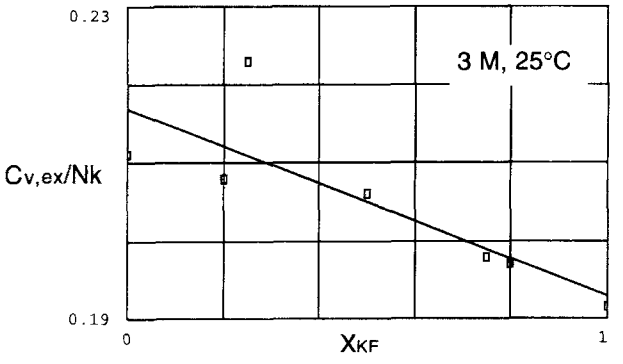

FIGURE 7 Harned plot of the dimensionless excess heat capacity at constant volume per ion as a function of the fraction of KF at 3 mol/L total concentration (25°C).

$$\ln y_{Cl^-}\,(\text{corr}) = -0.4588 + 0.0201\,X_{KF} \pm 0.0070\,(r = +0.6405) \quad (19)$$

$$\ln y_{F^-}\,(\text{corr}) = -0.2014 + 0.0742\,X_{KF} \pm 0.0020\,(r = +0.9951) \quad (20)$$

$$\ln y_{\pm}(\text{KCl, corr}) = -0.4602 + 0.1180\,X_{KF} \pm 0.0050\,(r = +0.9914) \quad (21)$$

$$\ln y_{\pm}(\text{KF, corr}) = -0.3330 + 0.1484\,X_{KF} \pm 0.0050\,(r = +0.9984) \quad (22)$$

The correlation coefficient is very good in most cases, but less good for $C_{V,ex}/Nk$ and $\ln y_{Cl^-}$(corr). In the latter case this is just because of scattering, since the variation of $\ln y_{Cl^-}$(corr) with salt fraction is very small. For $C_{V,ex}/Nk$, however, a parabola might be needed to fit the points. The best

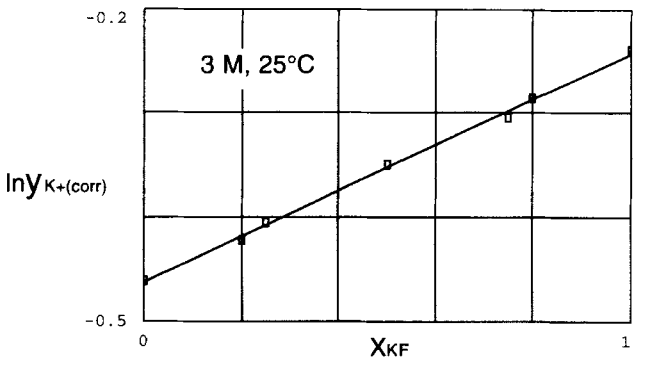

FIGURE 8 Harned plot of logarithm of the single ion activity coefficient of K^+ as a function of the fraction of KF at 3 mol/L total concentration (25°C).

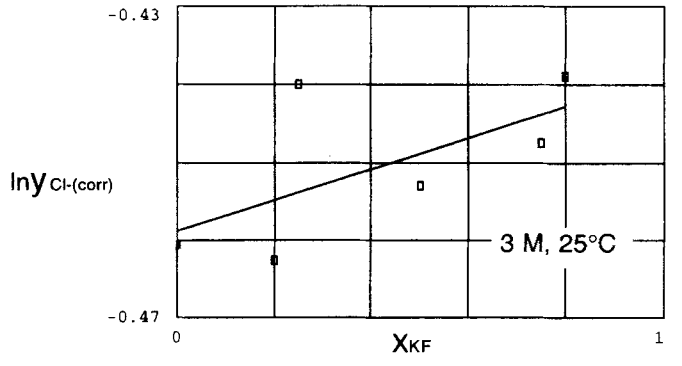

FIGURE 9 Harned plot of logarithm of the single ion activity coefficient of Cl^- as a function of the fraction of KF at 3 mol/L total concentration (25°C). The considerable scatter should be viewed in relation to the very small variation of the parameter in the whole range.

fitting least square parabola is:

$$C_{V,\mathrm{ex}}/Nk = 0.213 + 3.135 \cdot 10^{-3} X_{\mathrm{KF}} - 2.68 \cdot 10^{-2} X_{\mathrm{KF}}^2 \tag{23}$$

The two equations (21–22) may also be written in the traditional Harned's rule formulation

$$\ln y_{\pm}(\mathrm{KCl}) = \ln y_{\pm}(\text{pure KCl}) - \alpha^*_{\mathrm{KCl}} X_{\mathrm{KF}} \tag{24}$$

$$\ln y_{\pm}(\mathrm{KF}) = \ln y_{\pm}(\text{pure KF}) - \alpha^*_{\mathrm{KF}} X_{\mathrm{KCl}} \tag{25}$$

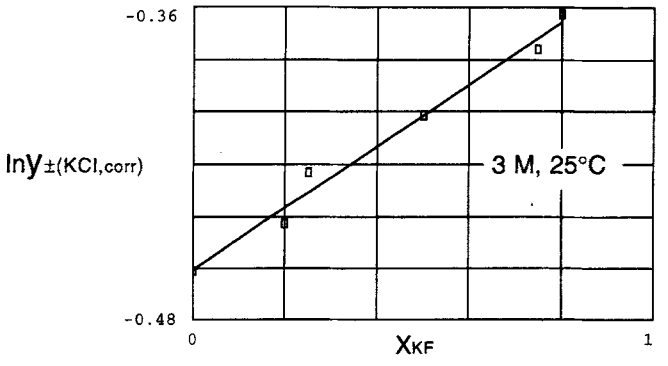

FIGURE 10 Harned plot of logarithm of the mean ionic activity coefficient of KCl in the mixtures as a function of the fraction of KF and 3 mol/L total concentration (25°C).

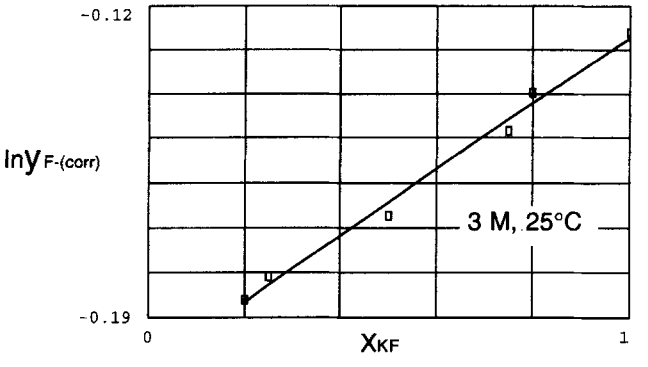

FIGURE 11 Harned plot of logarithm of the single ion activity coefficient of F^- as a function of the fraction of KF at 3 mol/L total concentration (25°C).

with

$$\ln y_{\pm}(\text{pure KCl}) = -0.460 \pm 0.005; \quad \alpha^*_{KCl} = -0.1180 \tag{26}$$

$$\ln y_{\pm}(\text{pure KF}) = -0.185 \pm 0.005; \quad \alpha^*_{F} \pm +0.1484 \tag{27}$$

The trace excess chemical potentials (divided by kT) are found inserting $X_{KF} = 1$ in Eq. (24) and $X_{KCl} = 1$ in Eq. (25):

$$\ln y_{\pm}(\text{trace KCl}) = -0.342 \pm 0.005;$$

$$\ln y_{\pm}(\text{trace KF}) = -0.333 \pm 0.005 \tag{28}$$

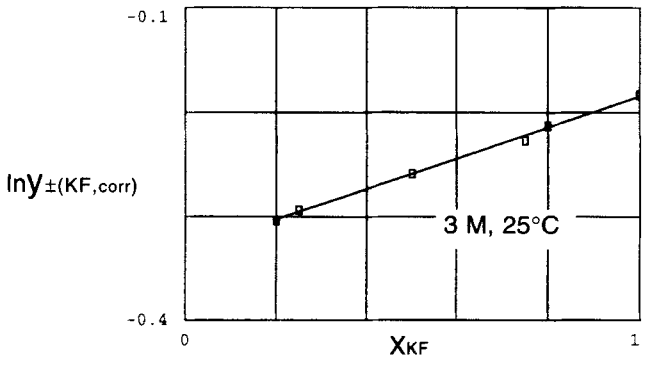

FIGURE 12 Harned plot of logarithm of the mean ionic activity coefficient of KF in the mixtures as a function of the fraction of KF at 3 mol/L total concentration (25°C).

The two trace excess chemical potentials are on the borderline of being identical within the uncertainty stated.

Mean Spherical Approximation (MSA) calculations have also been performed for the same system using the formalism stated in ref. [20]. From the calculated values the following perfect linear Harned expressions have been derived:

$$E_{ex}/NkT = -0.8595 + 0.05368\, X_{KF} \quad \text{(MSA)} \tag{29}$$

$$\ln y_{K^+}(\text{corr}) = -0.4567 + 0.2275\, X_{KF} \quad \text{(MSA)} \tag{30}$$

$$\ln y_{Cl^-}(\text{corr}) = -0.4567 + 0.04096\, X_{KF} \quad \text{(MSA)} \tag{31}$$

$$\ln y_{F^-}(\text{corr}) = -0.1836 + 0.07503\, X_{KF} \quad \text{(MSA)} \tag{32}$$

$$\ln y_{\pm}(\text{KCl, corr}) = -0.4567 + 0.1343\, X_{KF} \quad \text{(MSA)} \tag{33}$$

$$\ln y_{\pm}(\text{KF, corr}) = -0.3202 + 0.1513\, X_{KF} \quad \text{(MSA)} \tag{34}$$

Thus, we have

$$\ln y_{\pm}(\text{pure KCl,MSA}) = -0.4567; \quad \alpha^*_{KCl,MSA} = -0.1343 \tag{35}$$

$$\ln y_{\pm}(\text{pure KF,MSA}) = -0.1689; \quad \alpha^*_{KF,MSA} = +0.1513 \tag{36}$$

$$\ln y_{\pm}(\text{trace KCl,MSA}) = -0.3224; \quad \ln y_{+}(\text{trace KF,MSA}) = -0.3202 \tag{37}$$

The MSA values are surprisingly close to the MC values taking into account that the concentration is 3 M, and that it is generally believed that MSA calculations should be good only up to concentrations 1–2 M.

POTENTIALS OF MEAN FORCE

Figures 13–14 shows for a 3 M KCl solution the RDF's and the potentials of mean forces (obtained by logarithmation) as a function of ion separation in the simulation with $N = 64$ ions. The potentials of mean force have been multiplied by the dimensionless radial separation (t) for a better comparison

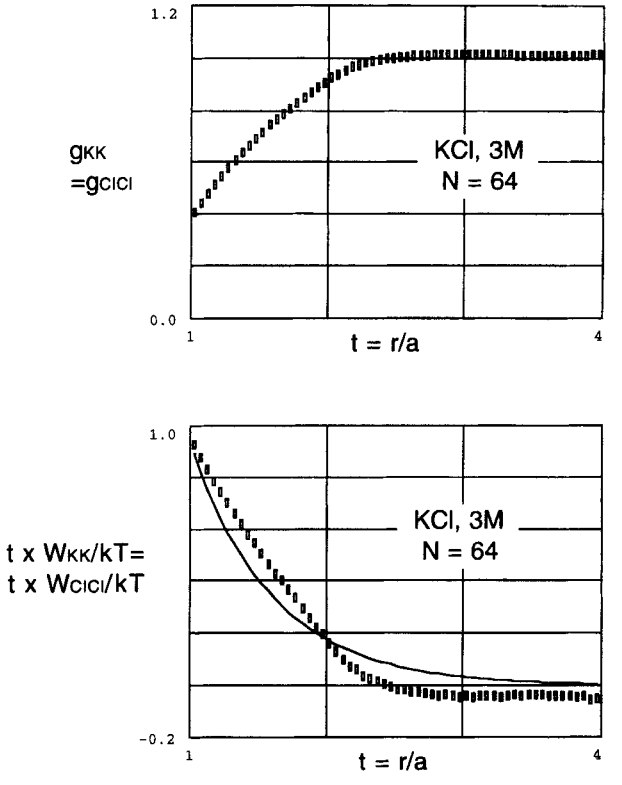

FIGURE 13 Above: Radial distribution function (RDF) between similar ions in pure 3 mol/L KCl. Below: Dimensionless potential of mean force (PMF) multiplied by the dimensionless radial separation (rectangles) compared to Debye-Hückel potential (solid curve).

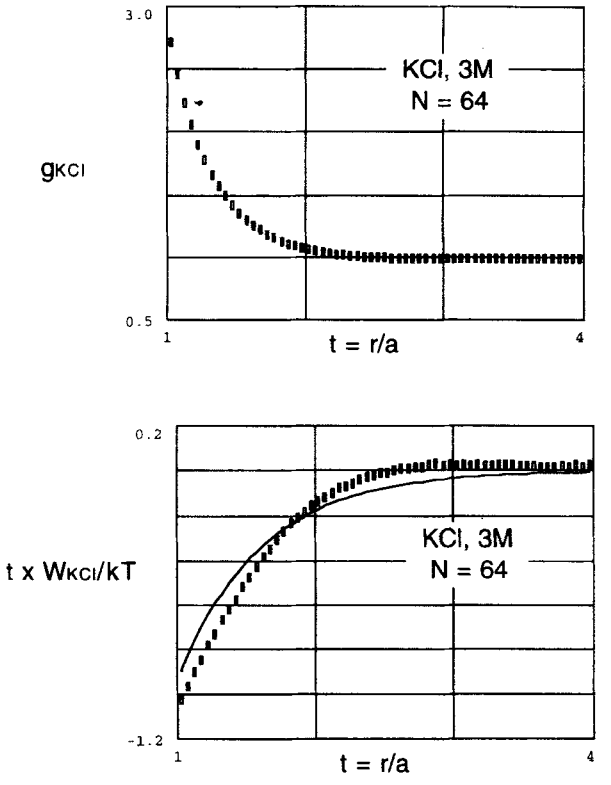

FIGURE 14 Above: RDF between K^+ and Cl^- in pure 3 mol/L KCl. Below: Dimensionless PMF multiplied by the dimensionless radial separation (rectangles) compared to Debye-Hückel potential (solid curve).

with the dimensionless Debye-Hückel potential:

$$[W_{+-}]_{DHX}/kT = (-B/t)\exp(\kappa a[1-t])/(1+\kappa a) \tag{38a}$$

$$[W_{++}]_{DHX}/kT = [W_{--}]_{DHX}/kT = (+B/t)\exp(\kappa a[1-t])/(1+\kappa a) \tag{38b}$$

The assumption that the potential derived from the linearized Poisson-Boltzmann equation may be used as an approximation for the potentials of mean force between the ions in a primitive electrolyte solution is usually called the DHX approximation. As we have seen in the previous papers, this approximation works quite well for the description of the RDF's even near to contact in dilute electrolytes where the Debye-Hückel linearisation is completely invalid. It also yields good results for the thermodynamic

properties up to $\kappa a \cong 0.3$. In all respects the DHX approximation is better than the simple DH approximation, which is in fact not a theory of high dilution but a theory valid in the limit $B \ll 1$.

Even at the present high concentration, where the Debye length is less than the ionic diameter ($\kappa a \cong 1.65$), Figures 13–14 shows that the DHX potentials of mean forces (curves) are quite good as "mean field approximations" for the real potential of mean forces (rectangles). They are not good enough to calculate thermodynamic properties, however. For the highest separations shown, the potentials of mean force (PMF's) are perturbed by the periodic boundary conditions (pbc's) and the Minimum Image (MI) energy cut-off as we shall shortly see in the following figures.

The PMF's in a 3 M KF solution are shown in Figures 15–17. Again, the DHX approximation delivers useful mean field approximations not too far from contact. In this case the Eq. (38b) are used for W_{KK} as well as for W_{FF}, and a is the mean ion diameter.

The PMF's in the "tails" of the distributions have been magnified in the lower figures in Figures 15–17. Two features are evident: (1) There is a perturbation from the pbc's and the MI since the simulations with $N = 216$ and $N = 100$ differ somewhat. (2) There is a certain "overshoot" in the PMF's, so that the potentials which are "attractive" for small separations are slightly "repulsive" at large separations and *vice versa.*

Considering first feature (1), the dimensionless half edge length of the simulation cell is $L/2 \cong 5.92$ for $N = 216$ and $L/2 \cong 4.58$ for $N = 100$. The latter value is not so much above the maximum separations in which the RDF's were sampled ($t \cong 4$). One effect of the perturbation from the pbc's and the MI seems to be an exaggeration of the "overshoot" phenomena.

The "overshoot" phenomenon is easily understood in the case of W_{KF}. Consider a "large" spherical part of the electroneutral solution with radius R and with a K^+ ion in the middle. Since there cannot be any excess of F^- ions in this sphere we have that the following second moment is equal to zero:

$$\int_{\text{contact}}^{R} (g_{KF}(t) - 1) t^2 \, dt = 0 \tag{39}$$

Evidently for this to be possible, the region near to contact where $g_{KF}(t) > 1$ has to be balanced by a region at larger separations where $g_{KF}(t) < 1$. For very large t values, $g_{KF}(t)$ tends to unity, of course. In case of identical ions

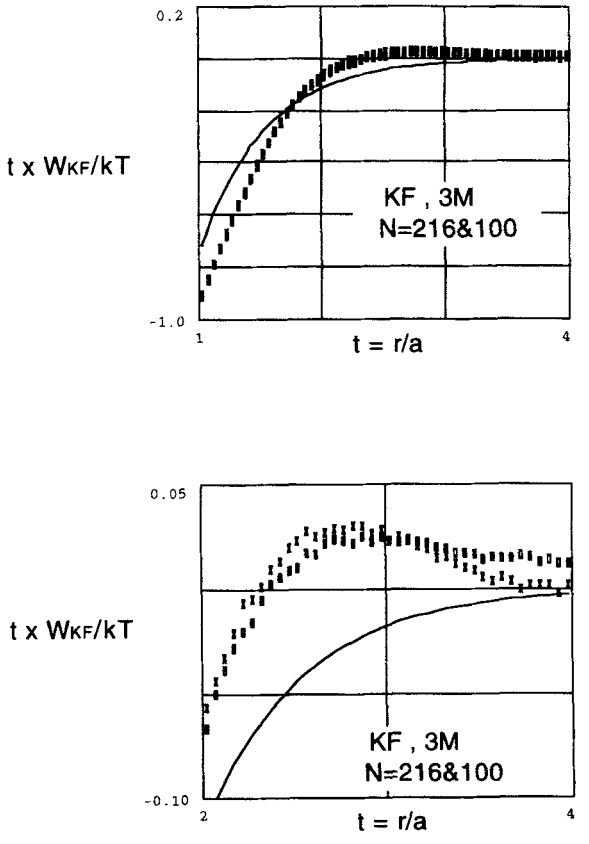

FIGURE 15 Above: Dimensionless PMF between K^+ and F^- in pure 3 mol/L KF multiplied by the dimensionless radial separation compared to Debye-Hückel potential (solid curve). Below: Magnification of the "tail' of the PMF multiplied by dimensionless radial separation compared to Debye-Hückel potential (solid curve). Rectangles: $N = 216$, 3×30 millions cf. Crosses: $N = 100$, 2×30 millions cf.

we have, for example,

$$4\pi\rho_K^* \cdot \times \int_{\text{contact}}^{R} (g_{KK}(t) - 1)\, t^2\, dt = -1 \tag{40}$$

since the central ion is lacking in the surroundings of the central ion. In this case there is no necessity of having a balancing region with $g_{KK}(t) > 1$ at higher t-values. Nevertheless there seems to be such a region if it is not a

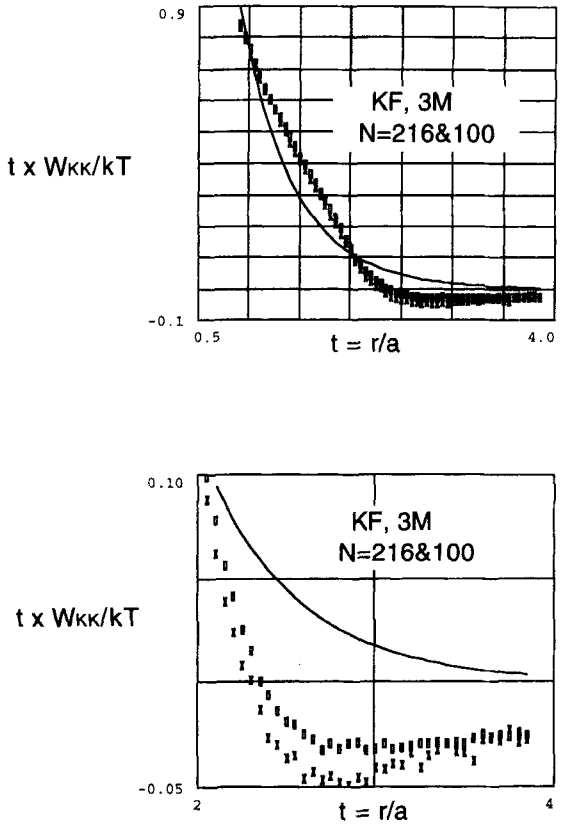

FIGURE 16 Above: Dimensionless PMF between K^+ and K^+ in pure 3 mol/L KF multiplied by the dimensionless radial separation compared to Debye-Hückel potential (solid curve). Below: Magnification of the "tail' of the PMF multiplied by dimensionless radial separation compared to Debye-Hückel potential (solid curve). Rectangles: $N = 216$, 3×30 millions cf. Crosses: $N = 100$, 2×30 millions cf.

result of the perturbations from the pbc's and the MI. This seems unlikely, however, in view of the results presented later with $N = 1000$.

In contrast, the DHX approximation is unable to describe the "overshoot" phenomenon. This approximation always yields monotonous RDF's and PMF's being wrong in the "far out tails".

We now pass to mixed electrolytes. Since we have 6 independent radial distribution functions in each simulation, we cannot present the results of all the simulations. We concentrate our efforts on the equimolar mixture ($X_{KF} = X_{KCl} = 1/2$) and the N-values 1000, 100 and 72. The half edge lengths in these three cases are $L/2 \cong 10.29$, 4.78 and 4.28, respectively. Thus, the RDF's at $t \cong 4$ are most probably perturbed by the pbc's and the MI in

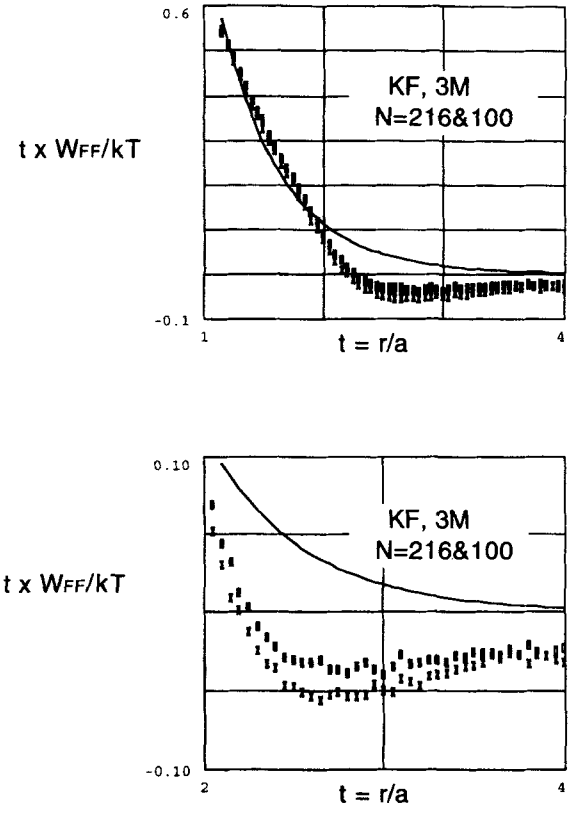

FIGURE 17 Above: Dimensionless PMF between F^- and F^- in pure 3 mol/L KF multiplied by the dimensionless radial separation compared to Debye-Hückel potential (solid curve). Below: Magnification of the "tail' of the PMF multiplied by dimensionless radial separation compared to Debye-Hückel potential (solid curve). Rectangles: $N = 216$, 3×30 millions cf. Crosses: $N = 100$, 2×30 millions cf.

the cases $N = 100$ and $N = 72$, whereas the $L/2$ for $N = 1000$ is more than the double of this maximum t-values sampled. In view of the very effective screening of the charges at this distance any perturbance should be nonexistent or very small.

Figures 18–23 shows the 6 PMF's (W_{KCl}, W_{KF}, W_{KK}, W_{ClCl}, W_{FF} and W_{ClF}) weighted by t as a function of separation. In all cases we have "overshoot" but closer to contact the DHX approximation is a mean field approximation. The two small systems ($N = 100$ and $N = 72$) are perturbed almost equally by the pbc's and MI, and the effect of the perturbation is to exaggerate the overshoot. However, a considerable overshoot is still observed for $N = 1000$ (rectangles), and these MC values are most probably very

close to the "real" values. The DHX approximation means here to use Eq. (38a) for all ions of opposite charges and Eq. (38b) for all ions of equal charges, with a being the mean diameter of the three ions. It is noteworthy that in many cases the PMF's at contact calculated by the DHX approximation are excellent approximations to the real ones.

ELECTRIC POTENTIALS AROUND IONS

The conditional electric potentials around the different types of ions-following one specific ion denominated the "central ion"-may be calculated *via* the

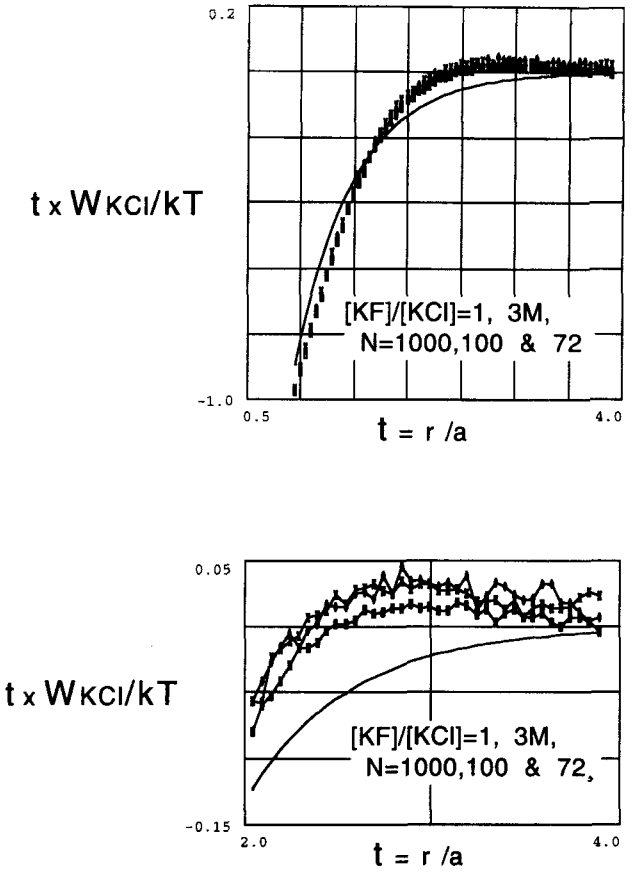

FIGURE 18 Above: Dimensionless PMF between K^+ and Cl^- in an equimolar mixture of KCl and KF at 3 mol/L total concentration multiplied by the dimensionless radial separation compared to Debye-Hückel potential (solid curve). Below: Magnification of the "tail' of the PMF multiplied by dimensionless radial separation compared to Debye-Hückel potential (solid curve). Rectangles: $N = 1000$. Diamonds: $N = 100$. Crosses: $N = 72$.

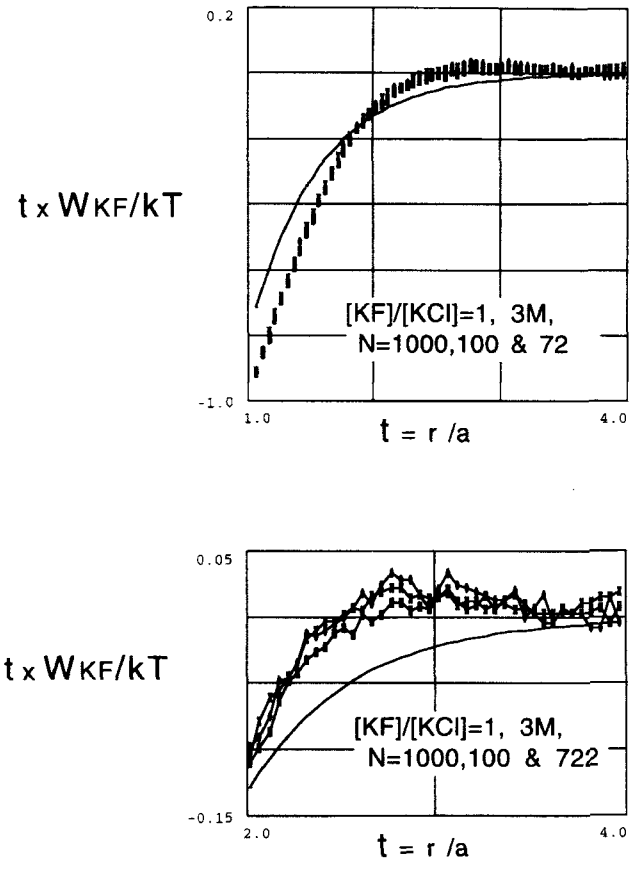

FIGURE 19 Above: Dimensionless PMF between K^+ and F^- in an equimolar mixture of KCl and KF at 3 mol/L total concentration multiplied by the dimensionless radial separation compared to Debye-Hückel potential (solid curve). Below: Magnification of the "tail' of the PMF multiplied by dimensionless radial separation compared to Debye-Hückel potential (solid curve). Rectangles: $N = 1000$. Diamonds: $N = 100$. Crosses: $N = 72$.

RDF's from which follows the conditional charge density around the central ion. Because of the spherical symmetry it is easy to perform a numerical integration of the equation of Poisson to obtain the electric potential. This programme was carried out by one of us for dilute 1:1 and 2:1 electrolytes and moderately concentrated electrolyte mixtures in earlier papers [6,8], and we use the formulas given in those papers. To our knowledge, the only previous attempt to calculate directly the electric potentials around ions was made in the very early MC study of Poirier [21]. He used very few ions and configurations, and the mean electric potential at fixed, equidistant

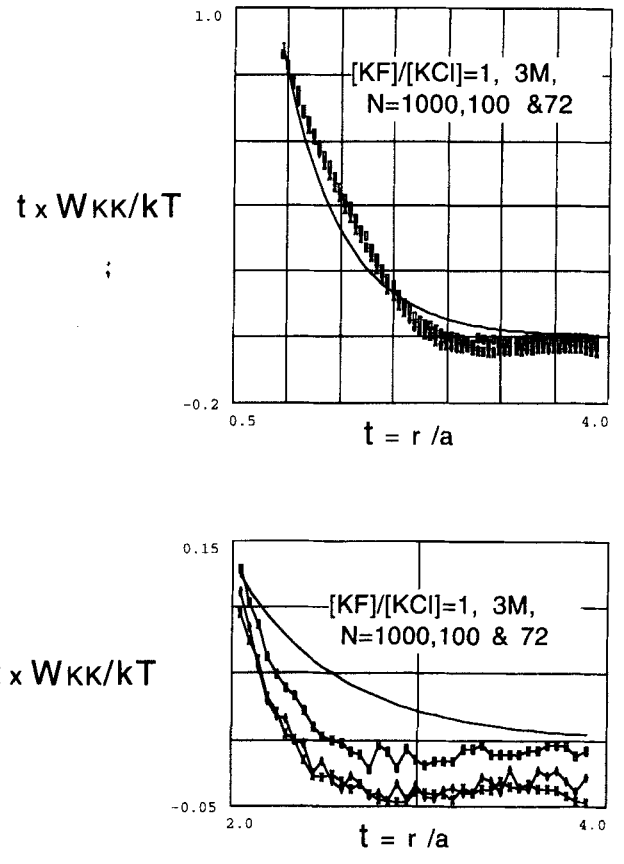

FIGURE 20 Above: Dimensionless PMF between K^+ and K^+ in an equimolar mixture of KCl and KF at 3 mol/L total concentration multiplied by the dimensionless radial separation compared to Debye-Hückel potential (solid curve). Below: Magnification of the "tail' of the PMF multiplied by dimensionless radial separation compared to Debye-Hückel potential (solid curve). Rectangles: $N = 1000$. Diamonds: $N = 100$. Crosses: $N = 72$.

points around a given fixed ion seemed to be directly sampled. Because of the Coulomb singularity met if the center one ion comes very close to a measuring point, this method appears somewhat questionable, however.

The electric potential is a *functional* of the complete, conditional charge distribution around the central ion. Since we can only sample the RDF's within a certain maximum distance, and since the pbc's and the MI energy cut-off may perturb the "tails" of the RDF's it is not possible to calculate the complete electric potential. It may be shown, however, that the *difference* in the electric potential relative to the potential at a maximum distance (t_{max}) may be calculated [6]. The value of t_{max} should not be so great, that

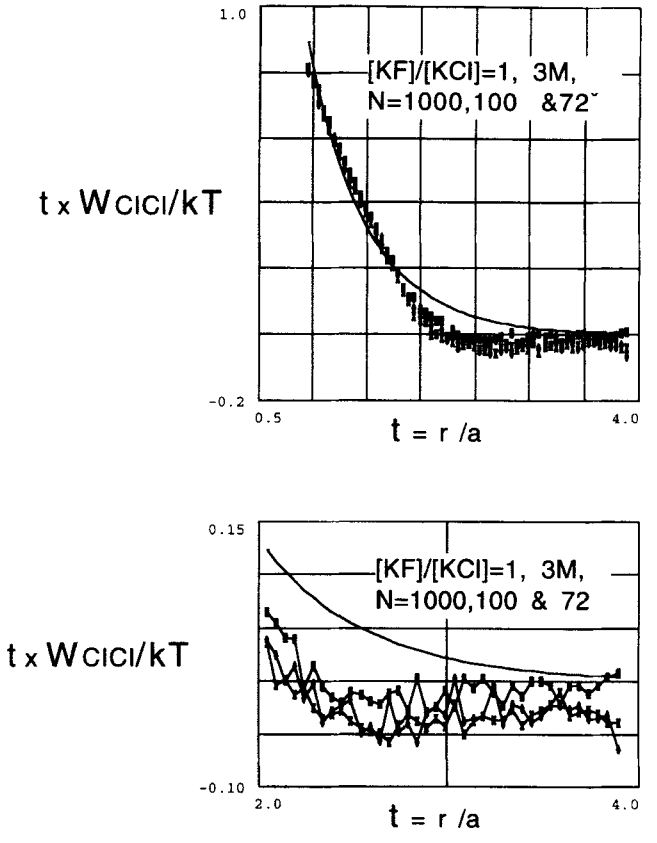

FIGURE 21 Above: Dimensionless PMF between Cl^- and Cl^- in an equimolar mixture of KCl and KF at 3 mol/L total concentration multiplied by the dimensionless radial separation compared to Debye-Hückel potential (solid curve). Below: Magnification of the "tail' of the PMF multiplied by dimensionless radial separation compared to Debye-Hückel potential (solid curve). Rectangles: $N = 1000$. Diamonds: $N = 100$. Crosses: $N = 72$.

the tail perturbations are important. Often, the value of t_{max} may nevertheless be taken big enough for the electric potential to be very small. The potential difference more close to the central ion will then be a very good approximation to the complete conditional potential.

By the designation $\Delta e_0 \Psi_{K^+}(t)/kT$ we mean for example:

$$\Delta e_0 \Psi_{K^+}(t)/kT = e_0 \Psi_{\text{around } K^+}(t)/kT - e_0 \Psi_{\text{around } K^+}(t_{max})/kT \qquad (41)$$

The $\Delta e_0 \Psi(t)/kT$ around either of the ions (with a change of sign only) in pure 3 M KCl is shown in Figure 24. The rectangles are the numerically

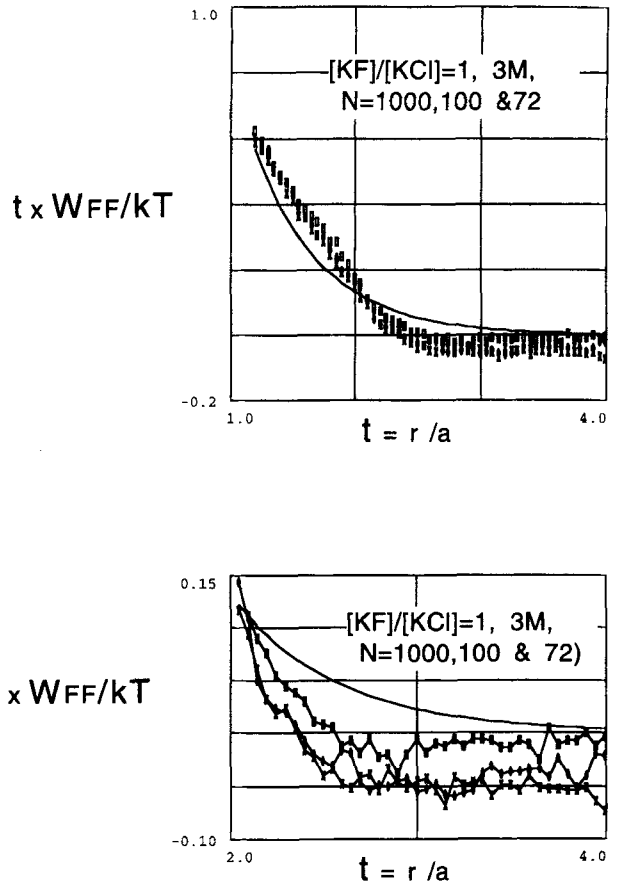

FIGURE 22 Above: Dimensionless PMF between F^- and F^- in an equimolar mixture of KCl and KF at 3 mol/L total concentration multiplied by the dimensionless radial separation compared to Debye-Hückel potential (solid curve). Below: Magnification of the "tail' of the PMF multiplied by dimensionless radial separation compared to Debye-Hückel potential (solid curve). Rectangles: $N = 1000$. Diamonds: $N = 100$. Crosses: $N = 72$.

calculated values. The number of ions in the simulation was 64 (the highest number used for the simulations of pure KCl, and the only one where $60 \times 0.05 + 1 = 4$ is less than $L/2$, see the section on methodology). The value of t_{max} was set to 2.975 only in order to avoid "tail perturbations".

The curve shown in Figure 24 corresponds to a "modified" Debye-Hückel expression:

$$\pm \Delta e_0 \Psi_{DH}(t)/kT = B\{[\exp(-\lambda at)/t] - [\exp(-\lambda at_{max})/t_{max}]\} \exp(\lambda a)/[1 + \lambda a] \quad (42)$$

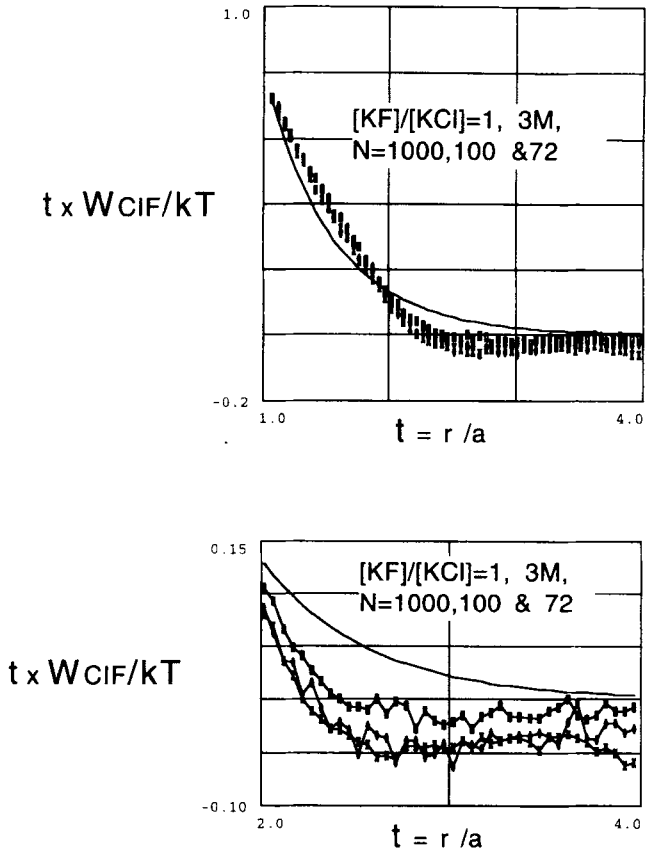

FIGURE 23 Above: Dimensionless PMF between Cl^- and F^- in an equimolar mixture of KCl and KF at 3 mol/L total concentration multiplied by the dimensionless radial separation compared to Debye-Hückel potential (solid curve). Below: Magnification of the "tail' of the PMF multiplied by dimensionless radial separation compared to Debye-Hückel potential (solid curve). Rectangles: $N = 1000$. Diamonds: $N = 100$. Crosses: $N = 72$.

where λ is an "effective inverse Debye length" which is in the present case 1.35 times the value of the real inverse Debye length of the system ($\kappa a \approx 1.65$). The fit is very good, though not perfect. This means, that the electrical potential distribution is close to be an eigenfunction to the partial differential equation

$$\nabla^2 \Psi = \lambda^2 \Psi \tag{43}$$

with a spherically symmetric Laplace operator. The eigenvalue is not the Debye-Hückel parameter κ^2, however. It is larger.

In 3 M KF, the electric potentials are shown in Figures 25–26. The mean of the three independent samplings of the RDF's with $N = 216$ have been used. The value of t_{max} was set to 3.353788 around the K^+ ion and 3.475 around the larger F^- ion. Fitting of eigenfunctions to Eq. (43) is somewhat less efficient in the tails than for KCl, especially around the F^- ion. Close to contact, however, the fit is quite good with $\lambda = 1.25\kappa$ for the K^+ ion and $\lambda = 1.90\kappa$ for the F^- ion ($\kappa a \approx 1.88$; κ is the same as for KCl, but the mean diameter a is greater for KF). There seems to be oscillations between negative and positive potentials far from the F^- ion.

The expression used to calculate the curves in Figures 25–26 is Eq. (42) with $a = 3.3$ nm, being the mean diameter of the two ions and with t measured relatively to this mean diameter. Consider the situation around a K^+ ion. The contact distance between the K^+ ion and other K^+ ions is 2.9 nm. Between 2.9 nm and 3.3 nm the only ions present are K^+coions, and the conditional charge density is positive. Above 3.3 nm there can also be F^- counterions, and these will dominate at short distances, so the charge density changes abruptly to negative values at a separation equal to 3.3 nm. This discontinuity has been carefully taken into account in the numerical integration of the Poisson equation. Nevertheless, the Debye-Hückel like potential near contact does not seem to be influenced by the discontinuity in the charge distribution.

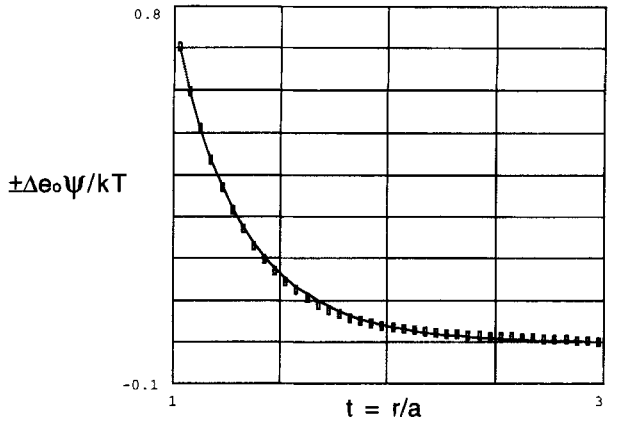

FIGURE 24 The difference in the dimensionless electric potential around an ion at the dimensionless radial separation t and the potential at $t_{max} = 2.975$. 3 mol/L pure KCl solution. The plus sign corresponds to the electric potential around the K^+ ion, the minus sign to the electric potential around the Cl^- ion. Rectangles: Calculated from Poisson integration of MC RDF's. Solid curve: Debye-Hückel eigenfunction with $\lambda a = 1.35\kappa a$ ($\kappa a = 1.650833$, $a = 0.29$ nm).

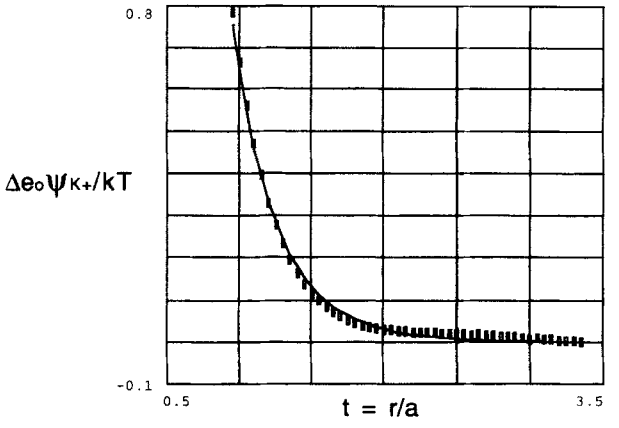

FIGURE 25 The difference in the dimensionless electric potential around the K^+ ion at the dimensionless radial separation t and the potential at $t_{max} = 3.353788$. 3 mol/L pure KF solution. Rectangles: Calculated from Poisson integration of MC RDF's. Solid curve: Debye-Hückel eigenfunction with $\lambda a = 1.25\kappa a$ ($\kappa a = 1.878505$, $a = 0.33$ nm).

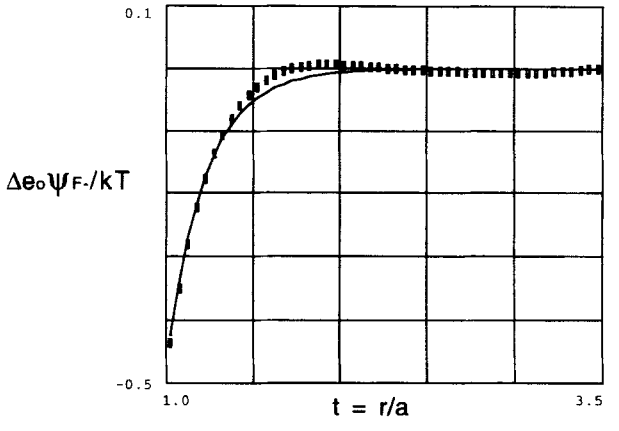

FIGURE 26 The difference in the dimensionless electric potential around the F^- ion at the dimensionless radial separation t and the potential at $t_{max} = 3.475$. 3 mol/L pure KF solution. Rectangles: Calculated from Poisson integration of MC RDF's. Solid curve: Debye-Hückel eigenfunction with $\lambda a = 1.90\kappa a$ ($\kappa a = 1.878505$, $a = 0.33$ nm).

Finally, Figures 27–29 shows the electric potential distribution around the three ions in a 3 M mixture with [KCl]/[KF] = 1. A total number of 1000 ions was used and t_{max} was set to 3.640789 around the K^+ ion and the Cl^- ion and to 3.767105 around the larger F^- ion. Simple DH eigenfuctions only fit close to contact with $\lambda = 1.50\kappa$ for the K^+ ion, $\lambda = 1.90\kappa$ for

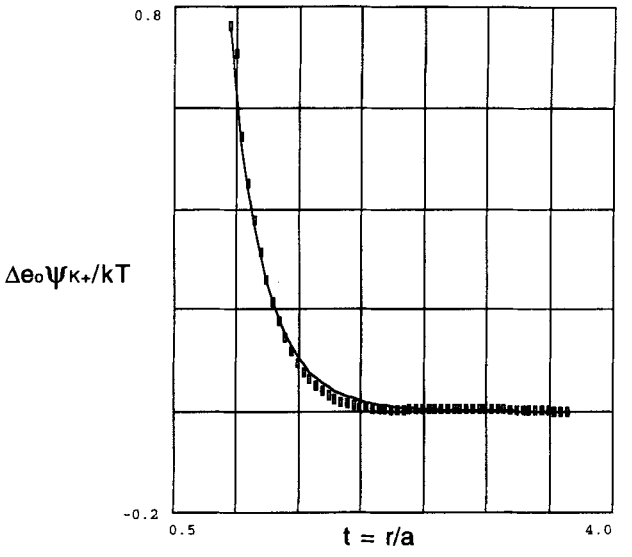

FIGURE 27 The difference in the dimensionless electric potential around the K^+ ion at the dimensionless radial separation t and the potential at $t_{max} = 3.640789$. 3 mol/L equimolar mixture of KCl and KF. Rectangles: Calculated from Poisson integration of MC RDF's. Solid curve: Debye-Hückel eigenfunction with $\lambda a = 1.50\kappa a$ ($\kappa a = 1.802444$, $a = 0.3166666....$ nm).

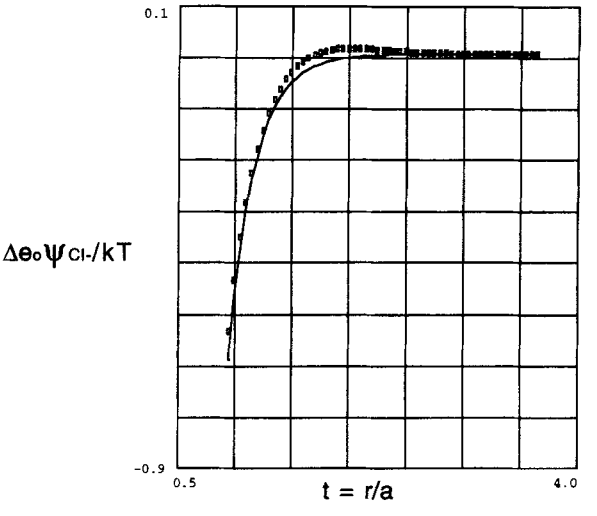

FIGURE 28 The difference in the dimensionless electric potential around the Cl^- ion at the dimensionless radial separation t and the potential at $t_{max} = 3.640789$. 3 mol/L equimolar mixture of KCL and KF. Rectangles: Calculated from Poisson integration of MC RDF's. Solid curve: Debye-Hückel eigenfunction with $\lambda a = 1.90\kappa a$ ($\kappa a = 1.802444$, $a = 0.3166666....$ nm).

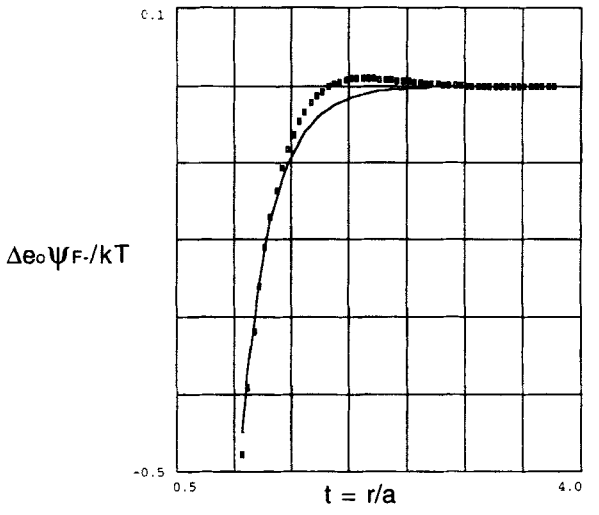

FIGURE 29 The difference in the dimensionless electric potential around the F^- ion at the dimensionless radial separation t and the potential at $t_{max} = 3.767105$. 3 mol/L equimolar mixture of KCl and KF. Rectangles: Calculated from Poisson integration of MC RDF's. Solid curve: Debye-Hückel eigenfunction with $\lambda a = 1.60\kappa a$ ($\kappa a = 1.802444$, $a = 0.3166666....$ nm).

the Cl^- ion and $\lambda = 1.60\kappa$ for the F^- ion ($\kappa a \approx 1.80$; κ is the same as for KCl and KF, but the mean diameter a is greater than in KCl and less than in KF). There is "overshoot" in the tails of the electric potentials around the two anions.

In Table IX we have collected the values for λ/κ for the potentials around the different ions in the three electrolytes at 2 M and at 3 M. The former values were given in ref. [8]. It should be noticed, that the fits of Debye-Hückel like eigenfunctions were considerably better in the tails for 2M electrolytes than in the case of 3M electrolytes. It is remarkable that the values of λ/κ for the K^+ ion in the two pure electrolytes seems independent of concentration, since the values for 2M and 3M are within the uncertainty of their determination. In contrast, the value of λ/κ for the F^- ion seems very sensitive to concentration changes. The same is the case for the Cl^- ion in mixtures.

CALCULATION OF THE EXCESS OSMOTIC PRESSURE

The excess osmotic pressure (the osmotic coefficient minus one) can be calculated from the excess energy and a "contact term" involving the RDF's

TABLE IX Values of λ/κ at 2 M and 3 M ionic strength

Electrolyte	*Concentration* *mol/L*	*Electric potential around* ..... K^+	Cl^-	F^-
KCl	2	1.38	1.38	–
KCl	3	1.35	1.35	–
[KCl]/[KF] = 1	2	1.27	1.50	1.33
[KCl]/[KF] = 1	3	1.50	1.90	1.60
KF	2	1.27	–	1.63
KF	3	1.25	–	1.90

The values corresponding to 2 M total concentration are taken from ref. [8], Table VII.

at contact. Let Π be the osmotic pressure and Π_{ex} the excess osmotic pressure (above the ideal, van't Hoff value). For a general primitive model electrolyte mixture with mean ion diameter = a the following relations hold true:

$$\prod_{ex}/(\rho_{tot}kT) \equiv \{\prod/(\rho_{tot}/kT)\} - 1 = E_{ex}/(3NkT) + \text{CONTACT} \quad (44)$$

$$\text{CONTACT} \equiv (2\pi/3)\sum_i\sum_j(\rho_i/\rho_{tot})(a_{ij}/a)^3\,\rho_j{}^*g_{ij}(\text{contact}) \quad (45)$$

To evaluate the RDF's at contact we have made plots of $t \cdot W_{ij}/kT$ *vs.* t for the four smallest values of t. The plots are perfectly straight lines (except for some scatter when RDF's between ions scarce in number are considered), and the extrapolation to contact is very safe. In Table X we have listed the contact values found from the simulations.

In Table XI the calculated excess osmotic coefficient and its components (electrostatic virial and contact term) are given as a function of the salt

TABLE X Contact values of the RDF's in 3M KCl/KF solutions

$\frac{[KCl]}{[KF]}$	N	$g_{KK}(cont)$	$g_{ClCl}(cont)$	$g_{FF}(cont)$	$g_{KCl}(cont)$	$g_{KF}(cont)$	$g_{ClF}(cont)$
∞	64	0.386(7)	0.386(7)	–	2.866(4)	–	–
4	1000	0.377(5)	0.386(9)	0.543(3)	2.949(7)	2.435(9)	0.480(6)
3	1000	0.378(3)	0.387(1)	0.561(0)	2.966(7)	2.448(7)	0.478(8)
1	1000	0.382(8)	0.397(9)	0.577(1)	2.997(0)	2.470(2)	0.493(8)
1/3	1000	0.378(4)	0.396(9)	0.596(1)	3.046(5)	2.527(2)	0.495(9)
1/4	1000	0.375(2)	0.395(4)	0.594(6)	3.055(8)	2.542(1)	0.495(2)
0	216	0.375(4)	–	0.606(4)	–	2.558(5)	–

The contact values have been obtained extrapolating the values of $t \cdot W_{ij}(t)/kT$ corresponding to the four smallest t-values to contact. Mostly, perfect linear regressions were seen with Pearson's r above 0.99.

TABLE XI Excess osmotic coefficient and its components in 3M KCl/KF solutions

X_{KF}	$E_{ex}/3NkT$	*CONTACT*	$\Pi_{ex}/\rho_{tot}kT$
0	−0.2909	0.300(3)	0.009(4)
0.2	−0.2871	0.325(4)	0.038(3)
0.25	−0.2862	0.331(7)	0.045(4)
0.5	−0.2815	0.359(1)	0.077(7)
0.75	−0.2768	0.391(4)	0.114(7)
0.8	−0.2758	0.398(3)	0.122(4)
1.0	−0.2721	0.423(4)	0.151(3)

fraction. It is seen that the two terms almost balance each other in the case of 3 M KCl, so that this solution is close to be "pseudo-ideal". With increasing fraction of KF the CONTACT contribution increases, however, and the repulsive hard sphere forces dominate to an increasing degree the net attractive electrostatic forces.

From Eq. (45) it is evident that the excess osmotic coefficient has quadratic terms in the salt fractions, and simple Harned linearity should not be expected for the osmotic coefficient. (The contact RDF's also varies slightly with the salt fraction). However, as was the case in 2M mixtures, the variation of the excess osmotic coefficient is not deviating very much from a linear variation with X_{KF}. The following quadratic, least square expression fits perfectly the simulation data:

$$\prod_{cx}/(\rho_{tot}kT) = 1.019 \cdot 10^{-2} + 0.13504 \cdot X_{KF} + 5.96 \cdot 10^{-3} X_{KF}^2 \qquad (46)$$

DISCUSSION

The linear Harned relations for the logarithm of the mean ionic activity coefficients in mixtures of 1:1 salts with constant total salt concentration are often written as follows:

$$\ln y_{\pm}(\text{salt1, mixture}) - \ln y_{\pm}(\text{pure salt1}, c_{tot}) = \alpha_{12} c_2 \qquad (47)$$

$$\ln y_{\pm}(\text{salt2, mixture}) - \ln y_{\pm}(\text{pure salt2}, c_{tot}) = \alpha_{21} c_1 \qquad (48)$$

The concentrations c_1 and c_2 are the salt concentrations and $c_{tot} = c_1 + c_2$. The coefficients α_{12} and α_{21} (with dimension of inverse concentration) are related to the dimensionless coefficients α^*_{12} and α^*_{21} of Eqs. (24–25) through

the equations:

$$\alpha^*_{12} = c_{\text{tot}}\alpha_{12}; \quad \alpha^*_{21} = c_{\text{tot}}\alpha_{21} \tag{49}$$

A plausible-though not unquestionable-explanation of the Eqs. (47–48) might be the following: We take the difference between the mean ionic chemical potential per salt molecule divided by $kT(\mu_{\pm}/kT)$ of the same salt in the mixture and in the a pure solution at the same total concentration. In this difference the standard chemical potential cancels out, and the differences is represented by the two left hand sides of Eq. (48). The electrostatic contribution to $\ln y_{\pm}$ (with a leading term proportional to $\sqrt{c_{\text{tot}}}$) is now supposed to be cancelled out in the difference, too. Then, at constant total concentration the differences $\ln y_{\pm}(\text{salt,mixture}) - \ln y_{\pm}(\text{pure salt}, c_{\text{tot}})$ is only affected by the amount of the second salt, and since the interaction is "chemical" rather than "electrostatic" ("specific interaction" in the words of an early work of Brønsted [22]) the leading term is of first order in the concentration of the second sal

It may be argued that the "electrostatic" and the "chemical" contributions to the activity coefficients are intrinsically interwoven except for the terms proportional to $\sqrt{c_{\text{tot}}}$, so that the exact cancellation of the electrostatic contributions mentioned is somewhat dubious. Furthermore, powers of higher orders than one in the salt concentration contribute to the $\ln y_{\pm}$ of the pure salts at higher concentrations and it is not strightforward to explain why only first order terms are necesary for the crossed interactions. Nevertheless, it is an experimental fact that many electrolyte mixtures follow linear Harned relations even at high total salt concentrations [23], and it is a theoretical fact that primitive model mixtures of "KCl" and "KF" obey linear mixing laws at 1M, 2M and 3M in the MSA approximation, in the symmetric Poisson-Boltzmann approximation as well as in more rigorous extrapolated Monte Carlo simulations [3,5,8,24].

Once the laws (47–48) are accepted-or the equivalent salt fraction laws Eqs. (24–25)-the other linear laws found for the excess energy, the $\ln y_i$ for the individual ions and (perhaps) for the excess osmotic heat capacity follow naturally by the same reasoning. The excess osmotic coefficient is in general quadratic in the salt fraction at constant total concentration. This follows from the theoretical expressions (44–45) as well as from a direct integration of the phenomenological equation for the variation in the osmotic pressure which we shall now perform.

First we have to state, however, that the primitive model treats the solvent as a "dielectric continuum". This is the first approximation one can do

to "solvent averaged" interionic forces, and thus the primitive model is in essence a McMillan-Mayer type of theory [25]. This means that the activity coefficients calculated are the ones found in the solution at a pressure equal to the external pressure plus the osmotic pressure, *i.e.* at constant solvent chemical potential. This should be contrasted to the normal Lewis-Randall activity coefficients at constant pressure and temperature.

For the changes in internal energy of our primitive model electrolyte mixture we write in general:

$$dU = TdS - pdV + \mu_{\pm}(\mathrm{KCl})\, dN_{\mathrm{KCl}} + \mu_{\pm}(\mathrm{KF})\, dN_{\mathrm{KF}} + \eta_{\mathrm{DC}}\, dV \qquad (50)$$

where η_{DC} is the chemical potential of one volume unit of dielectric continuum. Using the theorem of Euler we integrate Eq. (50) to

$$U = TS - pV + \mu_{\pm}(\mathrm{KCl})\, N_{\mathrm{KCl}} + \mu_{\pm}(\mathrm{KF})\, N_{\mathrm{KF}} + \eta_{\mathrm{DC}}\, V \qquad (51)$$

and by general differentiation of (51) and comparison with (50) we obtain the Gibbs-Duhem equation:

$$SdT - Vdp + N_{\mathrm{KCl}}\, d\mu_{\pm}(\mathrm{KCl}) + N_{\mathrm{KF}}\, d\mu_{\pm}(\mathrm{KF}) + Vd\eta_{\mathrm{DC}} = 0 \qquad (52)$$

Using the information that the temperature (T) and the "solvent" chemical potential (η_{DC}) is constant, and that the system pressure (p) is equal to the "external pressure" (p_{ex}) in the pure solvent-in equilibrium with the solvent through a hypothetical semipermeable membrane-plus the osmotic pressure in the salt solution (Π) we have from Eq. (52) dividing through by the volume (V):

$$d\prod = -dp_{\mathrm{ex}} + \rho_{\mathrm{KCl}}\, d\mu_{\pm}(\mathrm{KCl}) + \rho_{\mathrm{KF}}\, d\mu_{\pm}(\mathrm{KF}) \qquad (53)$$

The molecular densities of the salts are ρ_{KCl} and ρ_{KCl}. Fixing also the external pressure and considering only variations in composition at constant total salt density ($\rho_{\mathrm{tot}} = \rho_{\mathrm{KCl}} + \rho_{\mathrm{KF}}$) we have

$$d\{\prod/[kT\rho_{\mathrm{tot}}] - 1\} = X_{\mathrm{KCl}}\, d\ln\, y_{\pm}(\mathrm{KCl}) + X_{\mathrm{KF}}\, d\ln\, y_{\pm}(\mathrm{KF}) \qquad (54)$$

where the mean ionic activity coefficients are of the McMillan-Mayer type. Introducing now the Harned relations in the form of Eqs. (24–25) we obtain:

$$d\{\prod/kT\rho_{\mathrm{tot}}] - 1\} = -\alpha^{*}_{\mathrm{KCl}}\, dX_{\mathrm{KF}} + [\alpha^{*}_{\mathrm{KCl}} + \alpha^{*}_{\mathrm{KF}}]\, X_{\mathrm{KF}}\, dX_{\mathrm{KF}} \qquad (55)$$

We may integrate this equation from the "KCl end" ($X_{KF} = 0$) or from the "KF end" ($X_{KF} = 1$) to obtain the two expressions:

$$\{\prod_{ex}/kT\rho_{tot}]\} = \{\prod_{ex}/kT\rho_{tot}]\}_{KCl} - \alpha^*_{KCl} X_{KF} + (1/2)[\alpha^*_{KCl} + \alpha^*_{KF}] X_{KF}^2 \quad (56)$$

$$\{\prod_{ex}/kT\rho_{tot}]\} = \{\prod_{ex}/kT\rho_{tot}]\}_{KF} + (1/2)[\alpha^*_{KCl} - \alpha^*_{KF}]$$

$$- \alpha^*_{KCl} X_{KF} + (1/2)[\alpha^*_{KCl} + \alpha^*_{KF}] X_{KF}^2 \quad (57)$$

it is seen that the excess osmotic coefficient is only linear in the salt fraction if $\alpha^*_{KCl} + \alpha^*_{KF} = 0$.

In Figure 30 have plotted the excess osmotic coefficients calculated from the individual simulations *vs.* X_{KF} together with the least square quadratic (46) and the two curves (56–57). The two curves (56–57) deviate a little towards the end, where the excess osmotic coefficient is not fixed as an integration constant. These small deviations may be due to a lack of complete rigor of the linear Harned relations or-less likely-to some imprecision in the extrapolated MC data.

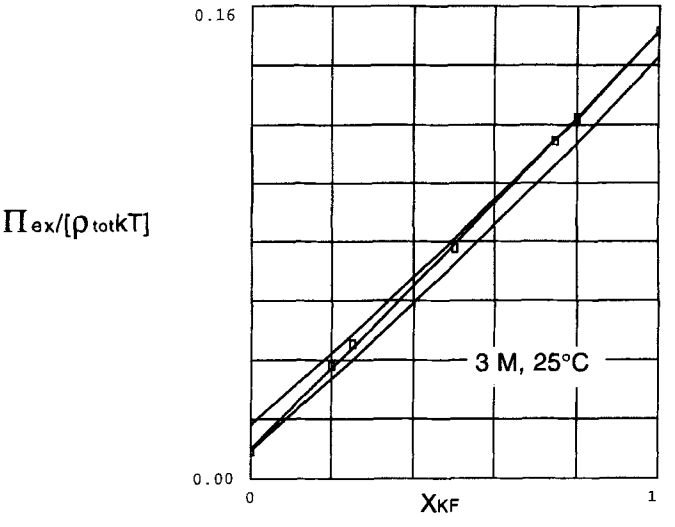

FIGURE 30 The excess osmotic pressure divided by the van't Hoff pressure = the excess osmotic coefficient as a function of the fraction of KF in mixtures of KCl and KF at 3 mol/L total concentration. Rectangles: Data calculated directly from MC data. Middle curve: Approximating least square parabola. Upper curve: Gibbs-Duhem integration from $X_{KF} = 1$. Lower curve: Gibbs-Duhem integration from $X_{KF} = 0$.

At 2 mol/L a salt fraction was found with pseudo-ideal behaviour. At this salt fraction, the net attractive, electrostatic forces and the excluded volume forces are in balance, and the osmotic pressure is the ideal, van't Hoff value. Enriching the solution with KCl (at constant total concentration) makes the attractive forces dominate (excess osmotic coefficient negative), whereas adding KF the excess osmotic coefficient become positive, because of the voluminous F^- ion. Increasing the total concentration displaces the excess osmotic coefficient *vs.* X_{KF} curve upwards (more excluded volume per L), and the pseudo-ideal point is displaced to the KCl side. At 3 mol/L the pseudo-ideal point has disappeared, but the pure KCl solution is close to be pseudo-ideal.

Comparing Eqs. (18–20) we see, that the coefficient of dependence of $\ln y_{Cl^-}$ on the salt fraction is only about 1/10 of the same coefficient for $\ln y_{K^+}$, and the coefficient for $\ln y_{F^-}$ about 1/3 of that for $\ln y_{K^+}$. Similar results were found by MC simulations at 1M [5] and 2M [8] "exaggerated" KF/KCl mixtures. These results bear some resemblance to the experimental findings of Bagg and Rechnitz [26]. Using EMF measurements with salt bridges these authors showed that the single-ion activity coefficient of the F^- ion in mixtures with trace concentrations of NaF in NaCl up to 1 mol/kg and in mixtures with trace concentrations of KF in KCl, KBr and KI up to 4 mol/kg were the same as in pure NaF, respectively pure KF solutions at the same concentrations.

According to the experimentally based speculations of Brønsted [22] concerning "specific interaction of ions" (the non-specific interactions are mediated through the ionic strength), these interactions should be more predominant between ions which has a great electrostatic likelihood to be in contact. Thus, the specific interaction is decreasing in the order K-Cl, K-F, F-F, F-Cl, {Cl-Cl & K-K}. Using this hypothesis, a tentative explanation of the very small varation of $\ln y_{Cl^-}$, the somewhat greater variation of $\ln y_{F^-}$, and the large variation of $\ln y_{K^-}$ has been given in Ref. [8].

Until now we have not explored the consequences of the Maxwell condition for the cross derivatives:

$$[\partial \ln y_{\pm}(\text{salt } 1)/\partial c_2]_{c_1,T,V,\eta_{DC}} = [\partial \ln y_{\pm}(\text{salt } 2)/\partial c_1]_{c_2,T,V,\eta_{DC}} \tag{58}$$

We shall do so following the procedure of McKay as described by Harned and Owen, Ref. [23], Chap. 14, section 10. However, we shall proceed further than this in deriving and solving a differential equation for $\alpha_{12} - \alpha_{21}$ as a function of c_{tot}. In the derivations in Ref. [23] the activity coefficients in Eq. (58) were meant to be Lewis-Randall activity coefficients so the condi-

tions were fixed T and p rather than fixed T, V and "solvent" chemical potential as in Eq. (58). That Eq. (58) is valid for the McMillan-Mayer activity coefficients in the primitive, electrolyte model is easily seen, however, introduing the modified, Helmholtz free energy:

$$F^* \equiv U - TS - \eta_{DC} V \tag{59}$$

we have

$$dF^* = -SdT - pdV - Vd\mu_{DC} + \mu_{\pm}(1)dN_1 + \mu_{\pm}(2)dN_2 \tag{60}$$

or-at constant V, T and μ_{DC}:

$$d(F^*/kTV)_{T,V,\eta_D} = [\mu_{\pm}^{id}(1)/kT + \ln y_{\pm}(1)]d\rho_1 + [\mu_{\pm}^{id}(2)/kT + \ln y_{\pm}(2)]d\rho_2 \tag{61}$$

Since F^*/kTV is a function of state, and since the cross derivatives are valid for the ideal dilute part of the chemical potentials, Eq. (58) follows immediately (changing from salt densities and chemical potentials per salt to molar concentrations and chemical potentials per mol).

As our point of departure for the use of Eq. (58) we suppose the Harned relations to be true. These may be written in two alternative forms:

$$\ln y_{\pm}(1, c_{tot}, c_1) = \ln y_{\pm}(1, \text{pure}, c_{tot}) - \alpha_{12}(c_{tot})\{c_{tot} - c_1\} \tag{62a}$$

$$\ln y_{\pm}(2, c_{tot}, c_1) = \ln y_{\pm}(2, \text{pure}, c_{tot}) - \alpha_{12}(c_{tot})\, c_1 \tag{62b}$$

$$\ln y_{\pm}(1, c_{tot}, c_2) = \ln y_{\pm}(1, \text{pure}, c_{tot}) - \alpha_{12}(c_{tot})\, c_2 \tag{63a}$$

$$\ln y_{\pm}(2, c_{tot}, c_2) = \ln y_{\pm}(2, \text{pure}, c_{tot}) - \alpha_{12}(c_{tot})\{c_{tot} - c_2\} \tag{63b}$$

From Eq. (58) and (62) we derive:

$$(\alpha_{12} - \alpha_{21}) + c_{tot} d\alpha_{12}/dc_{tot} - c_1 d(\alpha_{12} + \alpha_{21})/dc_{tot} = F(c_{tot}) \tag{64}$$

$$F(c) \equiv d \ln y_{\pm}(1, \text{pure}, c)/dc - d \ln y_{\pm}(2, \text{pure}, c)/dc \tag{65}$$

Since Eq. (64) has to be valid for any choice of (c_{tot}, c_1) and since all other terms than $c_1 d(\alpha_{12} + \alpha_{21})/dc_{tot}$ are only functions of c_{tot}, the latter term has to vanish, and we conclude (with McKay) that:

$$\alpha_{12} + \alpha_{21} = \text{constant (independent of } c_{tot}) \tag{66}$$

Thus, Eq. (64) can be rewritten as:

$$c_{\text{tot}} d\alpha_{12}/dc_{\text{tot}} + (\alpha_{12} - \alpha_{21}) = F(c_{\text{tot}}) \tag{67}$$

Using exactly the same procedures on the Eqs. (63a-b) we rederive the McKay relation and furthermore we have:

$$c_{\text{tot}} d\alpha_{21}/dc_{\text{tot}} - (\alpha_{12} - \alpha_{21}) = -F(c_{\text{tot}}) \tag{68}$$

Adding Eq. (67–68) we obtain $c_{\text{tot}} d(\alpha_{12} + \alpha_{21})/dc_{\text{tot}} = 0$, *i.e.* the McKay relation once more. Subtracting Eq. (67–68) we get the differential equation:

$$c_{\text{tot}} d\Delta\alpha/dc_{\text{tot}} + 2\Delta\alpha - 2F(c_{\text{tot}}) = 0 \tag{69}$$

$$\Delta\alpha \equiv \alpha_{12} - \alpha_{21} \tag{70}$$

Introducing

$$x \equiv \ln c_{\text{tot}} \tag{71}$$

$$G(x) \equiv F(c_{\text{tot}}) \tag{72}$$

Eq. (69) can be written as a linear, first order differential equation with one of the coefficients variable:

$$d\Delta\alpha/dx + 2\Delta\alpha - 2G(x) = 0 \tag{73}$$

This equation is solved by the method of substitution, see for example Ref. [27]. Eq. (73) is of the form $d\Delta\alpha/dx + P(x)\Delta\alpha + Q(x) = 0$ with $P(x) = 2$ and $Q(x) = -2G(x)$. We introduce the variable $u = \exp(\int P(x)dx) = \exp(2x)$ so that $P(x) = (1/u)du/dx$ and we integrate the equation $d\Delta\alpha/dx + (1/u)(du/dx)\Delta\alpha + Q(x) = 0$, or $d\{u\Delta\alpha\}/dx = -uQ(x)$ or in this case:

$$d\{\exp(2x)\Delta\alpha\}/dx = 2\exp(2x)G(x) \tag{74}$$

The solution is

$$\exp(2x)\Delta\alpha(x) - \exp(2x_0)\Delta\alpha(x_0) = 2\int_{\xi = x_0}^{x} \exp(2\xi)G(\xi)d\xi$$

or

$$\Delta\alpha(c_{tot}) = [c_0/c_{tot}]^2\Delta\alpha(c_0) + (2/c_{tot}^2)\int_{c=c_0}^{c_{tot}} cF(c)dc \tag{75}$$

where c_0 is a reference concentration where the linear Harned relations also hold true. Eq. (75) is an interesting *new* equation which-together with the McKay condition (66)-permits the calculation of the two Harned coefficients at any value of the total concentration if the values are given at one reference concentration. The only information needed is the concentration dependence of the activity coefficients of the pure electrolytes, and the only requirement is, that linear Harned rules are obeyed in the range of concentrations considered.

According to Harned and Owen, Ref. [23] Eq. (14–5–10), the so-called Åkerlöf-Thomas relation

$$\ln y_{\pm}(1, \text{pure}, c) - \ln y_{\pm}(2, \text{pure}, c) = B_{12}c \tag{76}$$

has been found experimentally to be approached at "high concentrations". In its original formulation, the activity coefficients are Lewis-Randall coefficients and the concentration is molality. In the present case we shall see, that the relation is excellent for the primitive model electrolytes investigated with McMillan-Mayer activity coefficients and c in mol/L, and that 1 mol/L is already serving as a "high" concentration.

Using the Åkerlöf-Thomas relation we see that $F(c) = B_{12}$, and inserting this relation into Eq. (75) we obtain:

$$\Delta\alpha(c_{tot}) = [c_0/c_{tot}]^2\Delta\alpha(c_0) + B_{12}\{1 - [c_0/c_{tot}]^2\} \tag{77}$$

It should be noticed, that it is a consequence of Eq. (77) that

$$B_{12} = \Delta\alpha(c_0) \Leftrightarrow \Delta\alpha(c_{tot}) = \Delta\alpha(c_0) \tag{78}$$

or in words: The difference between the Harned coefficients does not vary with the total concentration, if and only if the Åkerlöf-Thomas coefficient is equal to this difference. In that case, neither the sum nor the difference of the Harned coefficients vary, and both Harned coefficients are simply independent of c_{tot}. The above logicothermodynamical relations might be called the "theorem of invariance of the Harned coefficients". Perhaps this is natural to expect, since the Harned coefficients represent a linear perturbation

from the foreign salt and if so, there is a natural relation between the Åkerlöf-Thomas constant and the difference in the Harned coefficients (originating in the Maxwell cross differentiation conditions). In any case, as we shall see, the relation $\Delta\alpha = B_{12} = \text{constant}$ seems to be a good approximation in the present case.

The second column in Table XII shows the differences between the extrapolated MC values of $\ln y_{\pm}$ for pure KCl and $\ln y_{\pm}$ for pure KF at $c = 1$, 2 and 3 mol/L. The data are fitted very well by a least square straight line through the origin with slope $B_{12} = -0.0928$ L/mol, see the third column of Table XII. The fourth column shows the sum of the Harned coefficients. This sum seems not to be particularly constant. The values for 1 mol/L and 3 mol/L ar quite close, but the value for 2 mol/L only the half. However, since one Harned coefficient is positive and the other negative, and since they are approximately equal in absolute values, the sum of the Harned coefficients is a small and uncertain quantity given the "experimental" nature of the MC data. We shall "solve" this problem, as Alexander solved the Gordian knob problem by assuming:

$$\alpha_{KCl}(MC) + \alpha_{KF}(MC) = (0.009 \pm 0.004)\ \text{L/mol} \tag{79}$$

The differences $\alpha_{KCl}(MC) - \alpha_{KF}(MC)$ are given in the fifth column of Table XII. These differences are quite constant, and if we take the difference as (-0.88 ± 0.005) L/mol it is within the range of $B_{12} \approx -0.093$ L/mol, so the case seems to be quite close to the situation described by the "invariance theorem" stated in (78). In fact in the last column of Table XII, the difference between the Harned coefficients have been calculated at 1 mol/L and 3 mol/L from Eq. (77) using 2 mol/L as a reference, and there is practically no variation in this difference with c_{tot}. The somewhat lower value of the MC difference at 1 mol/L might be ascribed to the somewhat lower quality of these early simulation (in many of these simulations no more than 500,000 configurations were used). Probably, the "calculated" value of the

TABLE XII Åkerlöf-Thomas relation and properties of Harned coefficients for MC results

C_{tot} mol/L	$\ln y_{\pm}$ (pure KCl) $-\ln y_{\pm}$ (pure KF)	$B_{12} C_{tot}$ [a]	$\alpha_{KCl}+\alpha_{KF}$ L/mol	$\alpha_{KCl}-\alpha_{KF}$ L/mol	$\alpha_{KCl}-\alpha_{KF}$ [b] calculated L/mol
1	−0.096	−0.0928	0.010	−0.082	−0.093
2	−0.189	−0.1856	0.0048	−0.092	(−0.092)
3	−0.275	−0.2784	0.012	−0.089	−0.091

a) $B_{12} = -0.0928$ L/mol determined by least square line through (0, 0).
b) Calculated from Eq. (75) with $c_0 = 2$ mol/L and $F(c) = B_{12}$.

difference in Harned coefficients at 1 mol/L is closer to the truth than the direct MC value.

For comparison we show in Table XIII results completely similar to the ones in Table XII, but for the MSA calculations instead of the MC simulations. We see that the Åkerlöf-Thomas relation is less perfectly satisfied than for the MC results, though it is a fair approximation. The least square value of $B_{12} = -0.1032$ L/mol differs only a little from the MC value. The sum of the Harned coefficients tend to be closer to zero for the MSA values than for the MC values. However the relative variation is not less, and it is systematic in the total concentration in contrast to the erratic behaviour of the sum of the MC values. Since the MSA model always exhibits perfect Harned linearity at the three concentrations considered, the variation in the sum of the Harned coefficients with concentration can only be due to a certain thermodynamic *inconsistency* (*i.e.* disobeyance to the Maxwell rule) in the Mean Spherical *Approximation.*

The differences in the MSA Harned Coefficients vary only little with concentration, but the mean value is somewhat below the value of $B_{12} = -0.1032$ L/mol. The value calculated for the difference in Harned coefficients from Eq. (77) at 3 mol/L with $c_0 = 2$ mol/L deviates quite a lot from the MSA value, indicating an increasing thermodynamic inconsistency at the highest concentration.

Using the assumption (79) for the MC sum of Harned coefficients and the corresponding assumption

$$\alpha_{KCl}(\text{MSA}) + \alpha_{KF}(\text{MSA}) = (0.0043 \pm 0.0015)\ \text{L/mol} \tag{80}$$

together with the calculated differences from Eq. (77), both Harned coefficients may be calculated at 1 mol/L and 3 mol/L taking 2 mol/L as the concentration of reference. In Table XIV, the MC and MSA values of the Harned coefficient α_{KCl} are compared to the calculated values. These are

TABLE XIII Åkerlöf-Thomas relation and properties of Harned coefficients for MSA results

C_{tot} mol/L	$\ln y_{\pm}$ (pure KCl) $-\ln y_{\pm}$ (pure KF)	$B_{12} C_{tot}$ [a]	$\alpha_{KCl}+\alpha_{KF}$ L/mol	$\alpha_{KCl}-\alpha_{KF}$ L/mol	$\alpha_{KCl}-\alpha_{KF}$ [b] calculated L/mol
1	−0.0993	−0.1032	0.0029	−0.0919	−0.1001
2	−0.1894	−0.2064	0.0043	−0.0909	(−0.0909)
3	−0.3224	−0.3096	0.0056	−0.0952	−0.0755

a) $B_{12} = -0.1032$ L/mol determined by least square line through (0, 0).
b) Calculated from Eq. (75) with $c_0 = 2$ mol/L and $F(c) = B_{12}$.

well in accordance, except for the MC value at 1 mol/L which seems too low, and the "calculated" MSA value at 3 mol/L which also seems too low. As mentioned before, the simulations at 1 mol/L are not so extended as the simulations at the other two concentrations. The value "calculated" from the MC data at 2 mol/L is probably closer to the truth. The deviation of the calculated MSA value at 3 mol/L is due to the increase of inconsistency of this model at high concentrations.

Table XV displays similar results for the Harned coefficient α_{KF}. In this case, the only noteworthy deviation is the too low value calculated from the MSA model at 3 mol/L.

The ability of the MSA theory to reproduce quite well even such subtle quantities as the Harned coefficients which appear from comparison of the second and fourth colums of Tables XIV and XV is remarkable. For further comparison, Tables XVI and XVII show the MC and the MSA values of the ln $y_{\pm}$ of both salts in pure solutions and under trace conditions. The values calculated from the MSA theory are certainly without the range of probable values of the MC simulations (the cited value ± 0.005 is most probably larger than the real uncertainties in most cases). However, in view of its simplicity, the MSA seems a fair approximation for the activity coefficients even at 3 mol/L which is quite surprising, since the MSA theory is normally assumed to be valid only up to 1–2 mol/L for ordinary 1:1 electrolytes at 25°C.

Comparison of the fourth column in Table XVI with the same column in Table XVII shows that there is a quite good probability that the trace activity coefficients for the two salts are equal to each other at least at the two higher concentrations. Against this hypothesis is the fact, that the mean values of ln $y_{\pm}$(trace KCl) are invariably below the mean values of ln$y_{\pm}$(trace KF). At any rate the differences between the trace activity coefficients are very small.

TABLE XIV MC and MSA values of the Harned coefficient α_{KCl}

C_{tot} mol/L	$\alpha_{KCl}(MC)$ L/mol	$\alpha_{KCl}(MC, calc.)^{a)}$ L/mol	$\alpha_{KCl}(MSA)$ L/mol	$\alpha_{KCl}(MSA, calc.)^{b)}$ L/mol
1	−0.035	−0.042 ± 0.004	−0.0445	−0.0438 ± 0.0015
2	−0.0436	−0.042 ± 0.004	−0.0433	−0.0476 ± 0.0015
3	−0.0393	−0.041 ± 0.004	−0.0448	−0.0356 ± 0.0015

a) Calculated using $\alpha_{KCl} + \alpha_{KF} = 0.009 \pm 0.004$ L/mol and Eq. (75) with $c_0 = 2$ mol/L and $F(c) = B_{12} = -0.0928$ L/mol.
b) Calculated using $\alpha_{KCl} + \alpha_{KF} = 0.0043 \pm 0.0015$ L/mol and Eq. (75) with $c_0 = 2$ mol/L and $F(c) = B_{12} = -0.1032$ L/mol.

TABLE XV MC and MSA values of the Harned coefficient α_{KF}

C_{tot} mol/L	α_{KF} (MC) L/mol	α_{KF} (MC, calc.)[a] L/mol	α_{KF} (MSA) L/mol	α_{KF} (MSA, calc.)[b] L/mol
1	0.047	0.051 ± 0.004	0.0474	0.0481 ± 0.0015
2	0.0484	0.051 ± 0.004	0.0476	0.0476 ± 0.0015
3	0.0495	0.050 ± 0.004	0.0504	0.0399 ± 0.0015

a) Calculated using $\alpha_{KCl} + \alpha_{KF} = 0.009 \pm 0.004$ L/mol and Eq. (75) with $c_0 = 2$ mol/L and $F(c) = B_{12} = -0.0928$ L/mol.
b) Calculated using $\alpha_{KCl} + \alpha_{KF} = 0.0043 \pm 0.0015$ L/mol and Eq. (75) with $c_0 = 2$ mol/L and $F(c) = B_{12} = -0.1032$ L/mol.

TABLE XVI MC and MSA values of $\ln y_{\pm}$ (pure KCl) and $\ln y_{\pm}$ (trace KCl)

C_{tot} mol/L	$\ln y_{\pm}$ (pure KCl) MC	$\ln y_{\pm}$ (pure KCl) MSA	$\ln y_{\pm}$ (trace KCl) MC	$\ln y_{\pm}$ (trace KCl) MSA
1	-0.518 ± 0.005	-0.5145	-0.483 ± 0.005	-0.4700
2	-0.525 ± 0.005	-0.5158	-0.438 ± 0.005	-0.4293
3	-0.460 ± 0.005	-0.4567	-0.342 ± 0.005	-0.3224

TABLE XVII MC and MSA values of $\ln y_{\pm}$ (pure KF) and $\ln y_{\pm}$ (trace KF)

C_{tot} mol/L	$\ln y_{\pm}$ (pure KF) MC	$\ln y_{\pm}$ (pure KF) MSA	$\ln y_{\pm}$ (trace KF) MC	$\ln y_{\pm}$ (trace KF) MSA
1	-0.422 ± 0.005	-0.4152	-0.469 ± 0.005	-0.4626
2	-0.336 ± 0.005	-0.3264	-0.433 ± 0.005	-0.4215
3	-0.185 ± 0.005	-0.1343	-0.333 ± 0.005	-0.3202

The identity (or almost identity) of the two trace activity coefficients may be understood in terms of the "invariance theorem" stated in (78) and below. We have seen, that if the Harned coefficients are independent of concentration, we have $B_{12} = \alpha_{KCl} - \alpha_{KF}$. Since $B_{12} c_{tot} = \ln y_{\pm}(\text{pure KCl}, c_{tot}) - \ln y_{\pm}(\text{pure KF}, c_{tot})$ we have:

$$\ln y_{\pm}(\text{pure KCl}, c_{tot}) - \ln y_{\pm}(\text{pure KF}, c_{tot}) = (\alpha_{KCl} - \alpha_{KF})\, c_{tot}$$

or

$$\ln y_{\pm}(\text{pure KCl}, c_{tot}) - \alpha^*_{KCl} = \ln y_{\pm}(\text{pure KF}, c_{tot}) - \alpha^*_{KF}$$

or

$$\ln y_{\pm}(\text{trace KCl}, c_{tot}) = \ln y_{\pm}(\text{trace KF}, c_{tot}) \tag{81}$$

Thus, quite unexpectedly, the identity of the trace activity coefficients is a consequence of the concentration invariance of the Harned coefficients and the Åkerlöf-Thomas relation for the activity coefficients of the pure electrolytes!

If in addition we have the relation

$$\alpha_{KCl} + \alpha_{KF} = 0 \tag{82}$$

the common value of $\ln y_{\pm}$(trace) will be situated midway between $\ln y_{\pm}$(pure KCl) and $\ln y_{\pm}$(pure KF):

$$\ln y_{\pm}(\text{common trace}) = (1/2)[\ln y_{\pm}(\text{pure KCl}) + \ln y_{\pm}(\text{pure KF})] \tag{83}$$

Another consequence of Eq. (82) is, that the plot of the excess osmotic coefficient vs. the salt fraction of the mixture at constant total concentration will be perfectly linear and not quadratic, see Eq. (55). The relation (82) is found to be approximatively true for some electrolytes [23] and also in the present case case $\alpha_{KCl} + \alpha_{KF}$ seems to be an order of magnitude smaller than $\alpha_{KCl} - \alpha_{KF}$.

In the diagram Figure 31 we see how well the MC values of $\ln y_{\pm}$(trace KCl), $\ln y_{\pm}$(trace KF) and $[\ln y_{\pm}(\text{pure KCl}) + \ln y_{\pm}(\text{pure KF})]/2$

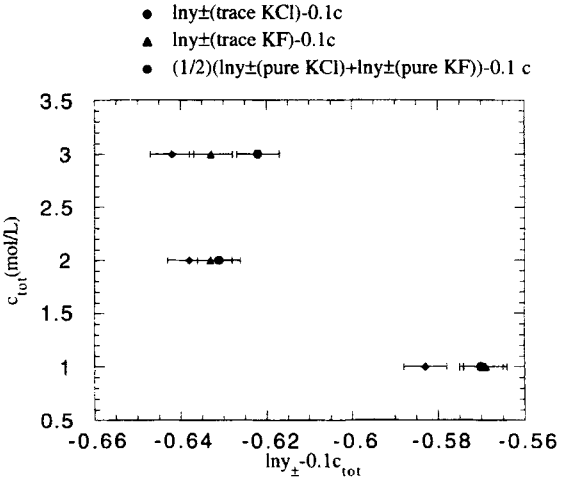

FIGURE 31 Uncertainty diagram showing if the MC values of $\ln y_{\pm}$(trace KCl) (diamonds), $\ln y_{\pm}$(trace KF) (triangles) and $[\ln y_{\pm}(\text{pure KCl}) - \ln y_{\pm}(\text{pure KF})]/2$ are identical or different at the three total concentrations 1, 2 and 3 mol L.

are separated at the total concentrations 1, 2 and 3 mol/L. At 2 mol/L the overlapping is so that Eqs. (81) and (83) might be true. At 1 mol/L ln $y_{\pm}$(trace KCl) is clearly different from [ln $y_{\pm}$(pure KCl) + ln $y_{\pm}$ (pure KF)]/2 and the trace activity coefficients are not equal. At 3 mol/L, the trace activity coefficients might be equal, but [ln $y_{\pm}$ (pure KCl) + ln $y_{\pm}$(pure KF)]/2 is clearly different. Also, many experimental measurements of Lewis-Randall activity coefficients in ternary mixtures show one or more of the following features: 1) Somewhat different trace activities, 2) $\alpha_{12} + \alpha_{21} \neq 0$ and 3) asymmetrically situated values of ln $y_{\pm}$(trace) [23].

Turning now our attention towards the structural properties of the solution, we have presented in selected cases the two properties which can be calculated from the sampled RDF's: The potentials of mean forces (PMF's) and the electric potentials around the three kinds of ions. Surprisingly, not too far from ion-ion contact the potential calculated from the linear, spherical Poisson-Boltzmann equation (the Debye-Hückel solution) is a fair mean field approximation even at 3 mol/L, as it was found to be also at 1 mol/L and 2 mol/L. In the "tails" of the PMF's, however, we have-as far as one might go out without having significant perturbations from the periodic boundary conditions-overshoot and undershoot phenomena which are foreign to the Debye-Hückel potentials.

For 1:1 and 2:1 electrolytes under dilute conditions the *electric potentials* around the ions-calculated from Poisson integration of the charge distributions-seem also to be described very well by the Debye-Hückel potentials even if the condition for the linearisation of the spherical Poisson-Boltzmann equation ($e_0\Psi / kT \ll 1$) is strongly violated close to contact [6]. Deviations from the Debye-Hückel electric potential are seen for dilute 2:2 electrolytes, and only small deviations are seen in some cases for "exaggerated" KF/KCl mixtures at 1 mol/l total concentration [6]. The reason for the "unreasonable" utility of the Debye-Hückel theory is, that the greatest contribution to the electric potential-even close to contact-comes from the relatively weakly charged, but voluminous, spherical shells at some distance from contact, where the linearisation condition *is* valid.

At 2 mol/L [8] and 3 mol/L, however, the Debye-Hückel potential ceases to fit the calculated electric potentials in KF/KCl mixtures. The mathematical form of the Debye-Hückel potential is still important, however, since a Debye-Hückel expression with an individual screening parameter (λ_i) for each ion (i) and for each given salt fraction fits the potentials quite well apart from minor oscillations and overshoot phenomena. The efficient screening parameters are always greater than the

Debye-Hückel parameter (κ), and the ratios (λ_i/κ) either stay approximately constant or grow when we increase the concentration from 2 mol/L to 3 mol/L, see Table IX.

The MC simulations for mixtures of univalent anions and cations of equal size with univalent anions of greater size are completely analogous to simulations of mixtures of univalent anions and cations of equal size with univalent cations of greater effective size, of course, for example KCl + HCl (the proton is strongly hydrated) or KCl + LiCl. The system investigated here may be taken as a model also for such systems. The MC analysis of this kind of systems is now quite complete. In the future it would be of interest to investigate 1:1:1 systems with three different ion diameters 1:1:1:1 systems (four different univalent ions) and 2:1:1 systems (for example $BaCl_2$ + HCl).

Acknowledgements

The authors are grateful for the financial support provided from the Dirección General de Investigación, Ciencia *y* Tecnología DGICYT (Madrid) under project PB92–0773-C03–03 and from financial support from BANCAJA under project P1B95–04. One of the authors is indebted to DGICYT for a sabbatical year guest professorship which enabled him to do research at Universitat Jaume 1, Castellón, Spain.

References

[1] Jensen, J. B., Jaskula, M. and Sørensen, T. S.(1987) "Mean activity coefficients in aqueous electrolyte mixtures. I. EMF studies at 25°C on the KCl-KF system", *Acta Chem. Scand.*, **A41**, 461.

[2] Sørensen, T. S. and Jensen, J. B. (1989) "Mean activity coefficients in aqueous electrolyte mixtures. II. The generalized DHX model and its resolution of seemingly paradoxical experimental results", *Acta Chem. Scand.*, **A43**, 421.

[3] Sørensen, T. S., Jensen, J. B. and Sloth, P. (1989) "Experimental activity coefficients in aqueous mixed solutions of KCl and KF at 25°C compared to Monte Carlo simulations and Mean Spherical Approximation calculations", *J. Chem. Soc. Faraday Trans. 1*, **85**, 2649.

[4] Sørensen, T. S. (1991) "Ions in solution and in a weak ion exchange membranes" in *Caplillarity Today. Lecture Notes in Physics, Vol. 386*, Pétré, G. and Sanfeld, A. eds., Springer-Verlag, Berlin-Heidelberg-New York-London-Paris-Tokyo-Hong Kong-Barcelona-Budapest, pp. 164–221.

[5] Sørensen, T. S. (1993) "High precision Canonical Ensemble Monte Carlo simulations of very dilute, primitive Z:Z and 2:1 electrolytes and of moderately concentrated 1:1 electrolyte mixtures", *Molecular Simulation*, **11**, 1.

[6] Sørensen, T. S. (1993) "Direct calculation of the electric potential distributions around ions from high precision Canonical Ensemble Monte Carlo simulations of some primitive model electrolyte systems", *Molecular Simulation*, **11**, 267.

[7] Sørensen, T. S. (1994) "What can be learned from Monte Carlo simulations of simple primitive model electrolyte systems?", *Trends in Chem. Engineering*, **2**, 543.

[8] Sørensen, T. S. (1995) "A very precise Canonical Ensemble Monte Carlo determination of thermodynamic properties and of radial distribution functions and electric potential around ions in primitive model 2 M mixtures of KCl and KF at 25°C", *Molecular Simulation*, **14**, 83.
[9] Skácel, F., Malmgren-Hansen, B., Sørensen, T. S., Jensen, J. B. (1990) "Electromotive force studies of cellulose acetate membranes. Binding of divalent cations and membrane potentials of KCl-KF mixtures", *J. Chem. Soc. Faraday Trans.*, **86**, 341.
[10] Metropolis, N., Rosenbluth, A. W., Rosenbluth, M. N., Teller, A. H. and Teller, E. (1953) "Equation of state calculations by fast computing machines', *J. Chem. Phys.*, **21**, 1087.
[11] Card, D. N. and Valleau, J. P. (1970) "Monte Carlo study of the thermodynamics of electrolyte solutions", *J. Chem. Phys.*, **52**, 6232.
[12] Sørensen, T. S. (1990) "How wrong is the Debye-Hückel Approximation for dilute primitive model electrolytes with moderate Bjerrum parameter?", *J. Chem. Soc. Faraday Trans.*, **86**, 1815.
[13] Sørensen, T. S. (1991) "Error in the Debye-Hückel Approximation for dilute primitive model electrolytes with Bjerrum parameters of 2 and ca. 6.8 investigated by Monte Carlo Methods. Excess energy, Helmholt free energy, heat capacity and Widom activity coefficients corrected for neutralising background", *J. Chem. Soc. Faraday Trans.*, **87**, 479.
[14] Widom, B. (1963) "Some topics in the theory of fluids", *J. Chem. Phys.*, **39**, 2808.
[15] Widom, B. (1982) "Potential-distribution theory and the statistical mechanics of fluids", *J. Phys. Chem.*, **86**, 869.
[16] Sloth, P. and Sørensen, T. S. (1988) "Monte Carlo simulations of single-ion chemical potentials. Preliminary results for the restricted primitive model", *Chem. Phys. Letters*, **143**, 140.
[17] Sloth, P. and Sørensen, T. S. (1988) "Monte Carlo simulations of single-ion chemical potentials. Results for the unrestricted primitive model", *Chem. Phys. Letters*, **146**, 452.
[18] Sloth, P. and Sørensen, T. S. (1990) "Monte Carlo calculations of chemical potentials in ionic fluids by application of Widom's formula: correction for finite-system effects" *Chem. Phys. Letters*, **173**, 51.
[19] MacQuarrie, D. A. (1976) Statistical Mechanics, Harper and Row, New York, 2nd edn. Chap. 13, section 13–4, Eqs. (41–43).
[20] Ebeling, W., Scherwinski, K. (1983) "On the estimation of theoretical individual activity coefficients of electrolytes. I Hard sphere Model", *Z. physikal. Chemie (Leipzig)*, **264**, 1.
[21] Poirier, J. C. (1966) "Current status of the statistical mechanical theory of ionic solutions" in *Chemical Physics of Ionic Solutions*, Conway, B. E. and Barradas, R. G. eds., Wiley, New York, pp. 9–28.
[22] Brønsted, J. N. (1921) "The principle of the specific interaction of ions", *Kgl. Danske Videnskab. Selskab, Mat.-Fys. Medd.*, **IV**, 4.
[23] Harned, H. S. and Owen, B. B. (1958)*The Physical Chemistry of Electrolytic Solutions*, 3rd Ed., Reinhold Publishing Corp., New York, Chap. 14.
[24] Molero, M., Outhwaite, C. W. and Bhuyian, L. B. (1992) "Individual ionic activity coefficients from a symmetric Poisson-Boltzmann theory, *J. Chem. Soc. Faraday Trans.*, **88**, 1541.
[25] McMillan, W. G. and Mayer, J. E. (1945) "The statistical Thermodynamics of Multicomponent systems", *J. Chem. Phys.*, **13**, 276.
[26] Bagg, J. and Rechnitz, G. A. (1973) "Single-ion activity of fluoride in mixed alkali halide solutions", *Analytical Chemistry*, **45**, 1069.
[27] Bartsch, H.-J. (1974) Matematische Formeln, VEB Fachbuchverlag, 14. Auflage Leipzig, sektion 8.2.3.